TECHNICAL NOTES

NATIONAL ADVISORY COMMITTEE FOR AERONAUTICS

No. 644

FLIGHT AND WIND-TUNNEL TESTS OF AN XBM-1 DIVE BOMBER

By Philip Donely and Henry A. Pearson
Langley Memorial Aeronautical Laboratory

Washington
April 1938

NATIONAL ADVISORY COMMITTEE FOR AERONAUTICS

TECHNICAL NOTE NO. 644

FLIGHT AND WIND-TUNNEL TESTS OF AN XBM-1 DIVE BOMBER

By Philip Donely and Henry A. Pearson

SUMMARY

Results are given of pressure-distribution measurements made in flight over the right wing cellule and the right half of the horizontal tail surfaces of a dive-bombing biplane. Simultaneous measurements were also taken of the air speed, control-surface positions, control forces, and normal accelerations during various abrupt maneuvers in a vertical plane. These maneuvers consisted of push-downs and pull-ups from level flight, dives and dive pull-outs, and push-ups from inverted flight.

In addition to the pressure measurements, flight tests were made to obtain (1) wing-fabric deflections during dives and (2) variation of the minimum drag coefficient with Reynolds Number. Supplementary tests were also made in the full-scale wind tunnel to obtain the characteristics of the airplane under various propeller conditions and with various tail settings.

The results indicate that: (1) By decreasing the fabric deflection between pressure ribs, the span load distribution was considerably modified near the center and the wing moment relations were changed; and (2) the minimum drag was less for the idling propeller than for the propeller locked in a vertical position. The value of $C_{D_{min}}$ was equal to $K(\text{Reynolds Number})^{-0.03}$ for a range from 2,800,000 to 13,100,000.

INTRODUCTION

This report summarizes the results of various tests of a Navy dive bomber conducted in 1933-34 by the N.A.C.A. at Langley Field, Va. These tests were made in accordance with requests from the Bureau of Aeronautics, Navy Department.

The primary objects were to obtain data on the wing load distribution, the structural deformations of the wing, the stresses in several wing members, and the tail loads in the maneuvers for which the airplane was designed. These data were then to be used by the Navy as a check on the structural-design requirements that had been established for this type of airplane. A secondary object was to determine the effect of the structural deformations on the load distribution by comparing the results from the critical maneuvers with results obtained at the same conditions of angle of attack but at such low air speeds that the loads and corresponding deformations would be negligible.

For a number of reasons these objectives were only partly attained. It was found that the bad vibration characteristics of the airplane, together with the relatively rigid wing structure, precluded obtaining sufficiently accurate wing-deflection measurements in flight to be of significance. Such deflection measurements were taken with a camera having multiple telephoto lenses. For the stress measurements, it was originally intended to use commercial magnetic-drive strain gages; these gages proved unsatisfactory, however, because of driving difficulties encountered as a result of the vibration.

Except for the failure to obtain the wing deformations and spar stress measurements, the objectives were attained. In addition to the pressure-distribution tests over wing and tail surfaces, a number of supplementary tests were made to obtain more information concerning interesting phenomena observed during the main test program.

APPARATUS

Airplane.- The airplane used in this investigation was a Martin XBM-1 airplane (fig. 1) modified at the factory from the regular service type (BM-1) as required by these tests. The essential characteristics of the airplane were not changed by the modifications, which consisted mainly of the permanent installation of special pressure ribs and pressure tubes, as well as the installation, in the fuselage, of instrument mounts that replaced the right fuel tank and service equipment in the rear cockpit. The dimensions of the XBM-1 pertinent to this report are given in table I.

The wing incidence may be taken as 0° over the greater portion of the span, as shown by measurements made from time to time during the tests. For the portion near the tip where rounding occurred, there was a gradual washout increasing from 0° to about 3° at the extreme tip. This twist resulted from the fairing of the tip sections during construction.

Instruments.- The following standard N.A.C.A. photographically recording instruments were used during the tests:

(a) One type 60 and two type 30 multiple recording manometers.

(b) Accelerometer.

(c) Air-speed recorder.

(d) Control-force recorder.

(e) Control-position recorder.

(f) Synchronizing timer.

(g) Inclinometer.

In addition to the foregoing instruments, a camera with multiple telephoto lenses and several magnetic-drive strain gages were used during some of the tests. The camera may be seen in figure 1 mounted in the rear cockpit with its lenses trained on source lights on the lower surface of the upper wing. As previously mentioned, however, the vibration and structural characteristics of this airplane prevented the obtaining of satisfactory records with the camera and the strain gages.

A pitot head, mounted on a boom about one chord length forward of the leading edge of the upper wing (see fig. 1) in order to reduce any interference error, was used to measure the air speed; it was calibrated in level flight.

Pressure ribs, tubing, and orifices.- The original installation of pressure ribs, tubing, and orifices in both wing and tail surfaces was made at the Martin factory in accordance with previous N.A.C.A. practice (reference 1). The orifice blocks for the wing pressure ribs were connected to the manometers by aluminum tubes and were secured to

rigid ribs at the locations shown in figure 2. Orifices at corresponding stations on the upper and lower surfaces of the wing were connected to opposite sides of the same pressure cell to give the resultant pressure at that station. Table II gives the location of these stations along the rib chords. Rubber tubes were used as connections between fixed and movable surfaces. The orifices in the corrugated-skin stabilizer were located so that the orifice openings were even with the crests of the corrugations and the whole surface was then covered with fabric. The smooth surface was provided to prevent local effects of the corrugations on the pressure measurements.

In the first installation, the wing fabric was secured to the pressure ribs only by the clamping action of the orifice caps. During preliminary dives, it was found that the fabric pulled loose at several of the orifices because of the magnitude of the pressures at such locations in combination with the relatively large wing-rib spacing. The original installation was then altered by enclosing each pressure rib in a tightly fitting fabric envelope to which the outer fabric was sewed along the entire rib length. With this installation, no pulling of the wing fabric could occur at the orifices and the true wing profiles were maintained at the pressure ribs.

Floating orifices.- Even though the profiles were maintained at the pressure ribs by the method employed, further tests indicated that the distributions measured at these sections might be considerably different from those occurring at unsupported sections. Accordingly, a single row of orifice blocks (rib G, fig. 2) was fastened directly to the fabric midway between two adjacent wing ribs on the lower wing.

Fabric-deflection recorders.- During some of the dives, the fabric deflection was measured at several spanwise stations by recording the travel of small wire pointers attached to the fabric inside the wing. The wires were restrained by guides to move vertically and made scratch records on smoked-glass plates attached to the wing spars.

METHOD AND TESTS

Preliminary tests.- Because of the experimental nature of the airplane and because of the severity of the

maneuvers to which it was ultimately to be subjected, several preliminary dives were first made to check the structural strength. These tests consisted of a series of dives gradually approaching terminal velocity and a 5g pull-out. These preliminary tests, as mentioned previously, showed the need for altering the method of fabric attachment and indicated that the fabric-deflection measurements and pressures over a floating rib would be of interest.

Wing pressure-distribution measurements in flight.- The flight tests consisted mainly of measuring the resultant pressure distribution over the right wing cellule and slipstream area during various maneuvers in a vertical plane. The maneuvers consisted of terminal-velocity dives, dive pull-outs, push-downs and pull-ups from level flight, and push-ups from inverted level flight. Thus the lift range was covered from maximum positive to maximum negative lift coefficients for the symmetrical-flight condition. Except for the dives and dive pull-outs, in which the engine was fully throttled, the flights were made with power on. In addition to the pressure distribution, simultaneous measurements were taken of the air speed, acceleration, control force, and control positions.

Pressure-distribution results from floating rib G, together with fabric-deflection measurements, indicated that the span loading would undoubtedly be wavelike, with the crests occurring at stations between ribs and the troughs at the wing and pressure ribs. The conditions obtained in flight on rib G were simulated by loading a portion of fabric. It was found that, although the fabric could sustain the required loads when relatively new, it might not do so after weathering. This fact was called to the attention of the Bureau of Aeronautics, Navy Department, with the result that the number of profile ribs on all airplanes of this type were doubled. This change was also made on the present airplane without disturbing any of the previous pressure ribs except rib D, which was moved over to position D' away from the proximity of the interplane struts (fig. 2); floating rib G was eliminated. Some of the previous tests were then repeated. In order to distinguish the data in this report, the results obtained before doubling the number of profile ribs are designated as those for "original" rib spacing as contrasted with those obtained later with the "modified" rib spacing.

Pressure distribution over the tail in flight.- The load distribution over the right half of the horizontal tail surfaces was measured in a few dive pull-outs and abrupt pull-ups from level flight. During these tests, simultaneous measurements were also taken of the control force, control position, air speed, and normal accelerations. The tests of the tail surface were made upon completion of the flight tests with the modified wing. The tubing from the orifices in the tail was faired around the monocoque fuselage and brought to the manometers, which were located in the rear cockpit. A portion of the installation may be seen in figure 1.

Wind-tunnel tests.- Upon the completion of the flight tests with the original rib spacing, the airplane was mounted in the full-scale wind tunnel and both force and pressure-distribution measurements were made. In the force tests, the lift and drag variation with the propeller removed was measured first with the horizontal tail surfaces removed and then with the surfaces in place for various elevator angles. Force tests were also made with tail surfaces in place for the case when the propeller was locked in a vertical position and also when the engine was operating with the throttle closed. Several additional flight tests were subsequently made for the purpose of extending the range of variation of $C_{D_{min}}$ with Reynolds Number when the propeller was locked and also when it was idling.

The pressure distribution of the wing was also measured in the wind tunnel when the propeller was locked and when the propeller was idling, with the horizontal tail surfaces in place. These pressure measurements were taken with the flight pressure-distribution installation that was already in the airplane.

PRECISION

Pressure measurements.- An appraisal of the precision of the wing forces measured by the instruments and the methods used in these tests is complicated by the wide range covered and by the impracticability of maintaining the optimum relation between instrument adjustment and test conditions. Although the error in the individual pressure is influenced by the sensitivity of the pressure cell and the location of the orifice, the absolute error

tends to remain constant, with the result that the relative error is small near the maximum instrument deflection. The estimated maximum absolute error in the individual pressure is no more than 3 pounds per square foot for the high-range cells, which, in general, were connected to orifices near the leading edges of the wing and the tail surfaces. This absolute error was about 1 pound per square foot for the low-range cells, which were generally used to record pressures near the trailing edges. The individual pressure records obtained for points located away from any disturbing area were generally smoother and more accurate than those near struts or in the slipstream.

Aside from errors in the individual pressures, errors due to fairing the rib pressure-distribution curves are of importance. The absolute error due to fairing, for a given shape of rib pressure-distribution curve, tends to be constant. There is, however, a tendency for the error to vary with the shape of the rib pressure curves and this error is least in the high-angle-of-attack condition. When these possibilities are taken into consideration, it is estimated that the load at any station along the span is accurate to within 10 pounds. The estimated error in total wing load or tail load is less than 100 pounds.

Other measurements.- The indicated air-speed measurements in steady conditions are believed to be accurate to within 1-1/2 miles per hour, as shown by several flights over a measured course. In accelerated maneuvers, such as in pull-ups, the error may be somewhat greater owing to the fact that the air-speed head is traveling at a different rate of speed from the wings.

Control-surface displacements, as given by the control-position recorder, are accurate to within $1/2^{\circ}$ and 2° for the stabilizer and elevator, respectively, and the control forces are correct to within 3 pounds. Normal accelerations are believed to be accurate to within 0.2g and longitudinal accelerations to within 0.1g.

RESULTS AND DISCUSSION

Wing pressure distribution.- Typical time histories of the results obtained during the flight tests are given in figures 3 to 13. Figures 3 to 6 are typical time histories of the variation of the over-all quantities during

dives and dive pull-outs, push-downs and pull-ups from level flight, and push-ups from inverted flight. Owing to the fact that the total wing loads are obtained by a relatively indirect process that involves much labor, they are generally given through a considerably shorter interval of time than the other records. Differences in the shape of the various time-history curves for the same type of maneuver are caused principally by differences in piloting technique, although modifying the rib spacing did effect a change in both the cellule moment relations and in the downwash at the tail. These changes appeared in the different stabilizer angles required for trimming the airplane, in the control force, and in the manner in which a dive pull-out was made with the modified wings.

Figures 7 to 13 show the variation of span loading corresponding to some of the runs given in figures 3 to 6. The span load curves, while showing a consistent trend within a given run, do not compare so well between the different runs. Since larger discrepancies may be present in any particular set of curves, real differences between the original and modified wing load distribution are difficult to detect from these figures and a method of averaging must be used. Average relations were obtained over each section by plotting the values of section normal-force coefficient against wing normal-force coefficients as given by

$$c_n = \frac{l}{qc} \quad \text{and} \quad C_N = \frac{L}{qS}$$

where c_n is the section normal-force coefficient.

C_N, wing normal-force coefficient.

q, dynamic pressure, pounds per square foot.

c, section chord, feet.

l, section load, pounds per foot of span.

S, wing area, square feet (measured to center line for upper wing, to wing root for lower wing).

L, integrated load acting on wing areas.

Figure 14 shows such a plot for section K and also

indicates the number of points used to establish each section curve. Each point was labeled for the type of maneuver in which it was obtained, so that any effect of wing distortion on the load distribution would be indicated by the tendency of points representing a given maneuver to be consistently either high or low with respect to those for steady flight. An examination of all the section c_n - wing C_N relations, similar to those given in figure 14, failed to show any such consistent trend in the section load curves, which inferred that for this airplane the cellule distortion was probably slight. The averaged curves of the variation of section c_n with wing C_N are shown in figures 15 and 16 for the original and modified wings, respectively. When these figures were plotted, the results for each rib were offset from those for adjacent ribs. The results given in figures 15 and 16 show that the main difference in the span loading between the original and modified wings (see fig. 17) occurs at the center section of the upper wing. This difference is a result of the greater ballooning of the fabric between ribs on the original wing, which essentially causes an increase in the camber, thereby increasing the lift. The effect of this change in camber is transferred through induction to an increase in load at the pressure ribs.

A method similar to that used to establish the section c_n - wing C_N relations was employed to obtain the average relations for the section pitching moment. These relations are given in figures 18 and 19 for the original and modified wings, respectively. The ordinates for these figures are the section pitching-moment coefficients about the wing leading edge (considering normal forces only) computed from the relation

$$c_m = \frac{M_{LE}}{qc^2}$$

where M_{LE} is the moment of the load diagram in pound-feet per foot. The slopes of these lines indicate the position of the aerodynamic center of the individual sections, and the intercept at zero section c_n gives the constant moment (c_{m_o}) about this center. The variation of the section pitching-moment coefficients and aerodynamic centers along the span is given in figure 20 where it can be seen that the effect of doubling the number of profile ribs was to reduce the pitching-moment coefficient as well as to

cause the section aerodynamic centers to move forward. These differences in the moment relations between the two wings are a further result of the difference in fabric deflection of the two wings.

Fabric-deflection measurements taken with the original wing during terminal-velocity dives indicated that the fabric bulged out about 1 inch at sections near the centers of the wing semispans, while at the center section of the upper wing the maximum bulge was more than 1-1/2 inches, which represented the maximum the gages could record. Figure 21 shows to scale the envelope of the fabric deflections measured near the floating rib G during a mild pull-out from a terminal-velocity dive. At low lift coefficients the measured bulge at the nose is particularly interesting since it may have had a considerable effect on the value of the wing $C_{D_{min}}$. If fabric deflections had been measured at large loads for a high-angle-of attack condition, the deflection envelope might also have indicated an outward bulge on the upper surface of the leading edge.

The effect of the fabric lift on the section characteristics, such as c_n and c_m, is shown in figure 22, where the results for floating rib G are compared with those for the adjacent fixed pressure rib K. These comparisons cover only a limited range, since the pressure distribution over rib G was measured for relatively few dives and dive pull-outs. Since the normal accelerations were held below 5g, the limiting value, the maximum wing normal-force coefficients measured in the dive pull-outs were never more than 0.3.

Other over-all quantities obtained from the wing pressure-distribution tests are shown in figures 23 to 25. Figure 23 shows a comparison of the measured relative lift distributions for the original and modified wings with the relative distribution computed by using the method of reference 2. The values of the experimental points have been determined from the relations

$$C_{N_U} = \frac{L_U}{qS_U} \qquad C_{N_B} = \frac{C_{N_U} S_U + C_{N_L} S_L}{S_U + S_L}$$

where L_U and L_L are the integrated loads for upper and lower wings, pounds.

S_U and S_L, the upper and lower wing areas, square feet. Lower wing area does not include the part intercepted by the fuselage.

It can be seen that the results obtained by the method of reference 2 are in good agreement with experimental results.

The relation of the wing pitching-moment coefficient to the wing normal-force coefficient is given in figure 24; figure 25 shows the variation of lateral centers of pressure for the wings. As would be expected from the previous rib-pressure results, the pitching-moment coefficients at zero lift for the wing are slightly greater with the original rib spacing. The pitching-moment coefficients for the lower wings appear to be slightly larger than those for the upper wings, which is a common trait exhibited by biplane arrangements with conventional amounts of positive stagger.

The lateral centers of pressure (fig. 25) show only minor changes when a comparison is made between the original and modified wings. For both the upper and lower wings, the center of pressure remains inboard of the 50-percent point over the larger part of the lift range.

Full-scale-tunnel tests.- Although the average pressure-distribution measurements obtained in the tunnel agreed fairly well with those obtained in steady flight, the scatter of points determining the individual section c_n - wing C_N curves was greater. This increased scatter was due in part to the slight changes in flow angularity with tunnel speed and in part to the fact that the flight instruments were not sufficiently sensitive for operation at the low air speeds used during part of the wind-tunnel tests. The tunnel speeds ranged from approximately 50 to 110 miles per hour, the higher speeds being used at the low angles of attack.

Typical results from the wind-tunnel force tests are shown in figures 26 and 27. Figure 26 gives the variation of airplane lift and drag coefficients with angle of attack for the propeller removed. The various curves show the effect of the presence of the horizontal tail surfaces and of

the elevator deflection with zero stabilizer angle. The coefficients are based on an effective wing area of 429 square feet, which includes the wing area intercepted by the fuselage. The effect of the propeller on the force-test characteristics was indicated principally in the value of the airplane minimum drag coefficient. This variation is summarized in figure 27 and table III for a range of Reynolds Number from 2.8×10^6 to 13.1×10^6 with various propeller conditions. Several flight-test points obtained from terminal-velocity dives are included. For the locked-propeller dive, the airplane was fitted with a brake that held the propeller in a vertical position.

It can be seen from figure 27 that for this airplane the propeller (operating at negative thrust) has less drag when idling than when locked in a vertical position. This result is for a fixed blade angle of 15.4° at 0.75 R. Figure 27 also indicates that the propeller drag is anywhere from 10 to 16 percent of the total airplane drag at the low lift coefficients encountered in the dive and that, for the range tested, the variation of $C_{D_{min}}$ with Reynolds Number occurs according to $C_{D_{min}} = K R^{-0.03}$. This relationship, of course, applies only to the range tested and is applicable only to this particular type of airplane.

Tail-surface pressure distribution.- Results of the pressure-distribution tests on the tail are shown in figures 28 to 31. Figure 28 shows typical time histories of the quantities measured in abrupt pull-ups from level flight and figure 29 shows typical time histories of dive pull-outs. For the pull-ups (fig. 28), the measured normal acceleration varies directly with initial air speed in spite of a tendency for the elevator deflection to be less at the higher speeds. In practically all of the pull-up tests, the pilot exerted a maximum increment of force of about 120 pounds applied in a period of about 0.2 second. For the vertical dives, it can be seen that the pilot generally made the pull-out (fig. 29) by simply relieving the push on the stick, rather than by exerting a definite pull on the stick as was done in the pull-ups. In the present case, the necessary increase in the airplane pitching moment required to cause the pull-out is brought about by a change in the tail rib-load distribution, as the total down tail load is actually decreased in order to pull out of the dive. This fact is indicated clearly in the lower

curves of figure 29, where the history of the variation of tail load and of the tail pitching-moment coefficient for the right half of the horizontal tail surfaces is shown.

The differences between the chord-load distribution in an abrupt pull-up from level flight and for the dive pull-out may be seen by comparing the rib-load curves of figure 30. These curves correspond to runs previously shown in figures 28 and 29. Although the maximum tail loads of figure 30 are of the same order of magnitude (555 pounds for the pull-out, 510 pounds for the pull-up), the section distributions indicate clearly that two distributions must be used in the design of the horizontal tail surfaces.

The load distribution across the span varied with the type of maneuver, as may be seen from figure 31, which gives the spanwise-load distributions corresponding to the maximum loads indicated by the runs given in figures 28 and 29. The difference in the shapes of the span-load curves (fig. 31) is probably due either to a change in the shape of the downwash distribution from the wing or to the different thrust conditions encountered in the dive pull-outs and pull-ups from level flight.

CONCLUDING REMARKS

The effect of the greater fabric deflection of the wings with the wide profile rib spacing was to increase the section pitching moments along the span and to move the section aerodynamic centers rearward. For airplanes with fabric-covered wings that are required to operate at high speeds, it is necessary from both aerodynamic and structural considerations to prevent excessive fabric deflection.

The method of reference 2 for computing the division of the lift between wings gave good agreement with the experimental results except near zero lift.

In the pull-ups from level flight, the necessary increments in pitching moment were supplied by an increase in the down tail load; whereas, in the dive pull-out, the increase in moment was produced by a change in distribution with the down load on the tail actually decreasing. This result indicates clearly the necessity of designing

the tail on this type of airplane for different rib-load distributions.

Drag measurements showed that the idling propeller gave less drag than the propeller locked in a vertical position and that the propeller drag amounts to from 10 to 16 percent of the total drag in the dive. The minimum drag coefficient of this airplane with the propeller either locked or idling is equal to $K R^{-0.03}$ for a range of Reynolds Numbers from 2,800,000 to 13,100,000.

Langley Memorial Aeronautical Laboratory,
National Advisory Committee for Aeronautics,
Langley Field, Va., January 17, 1938.

REFERENCES

1. Rhode, Richard V.: The Pressure Distribution over the Wings and Tail Surfaces of a PW-9 Pursuit Airplane in Flight. T.R. No. 364, N.A.C.A., 1930.

2. Diehl, Walter S.: Relative Loading on Biplane Wings. T.R. No. 458, N.A.C.A., 1933.

TABLE I

CHARACTERISTICS OF THE XBM-1 AIRPLANE

Engine, P. & W. R1690-C	575 hp. at 2,100 r.p.m. at 7,500 ft.
Propeller:	
Diameter	10 ft.
Blade angle at 0.75 R	15.4°
Weight during flight tests	5,800 lb.
High speed at 6,000 feet	131 m.p.h.
Stalling speed	59 m.p.h.
Areas:	
Upper wing (including ailerons)	231 sq. ft.
Lower wing (including ailerons)	181 sq. ft.
TOTAL	412 sq. ft.
Stabilizer (both halves)	29.3 sq. ft.
Elevator (both halves)	27.4 sq. ft.
TOTAL	56.7 sq. ft.
Lengths:	
Span upper wing	41.0 ft.
Span lower wing	40.0 ft.
Chord upper wing	74 in.
Chord lower wing	65 in.

TABLE I - (Cont.)

Lengths (cont.):	
Center-of-gravity location for wing tests (back of leading edge of lower wing)	9.6 in.
Center-of-gravity location for tail tests (back of leading edge of lower wing)	9.2 in.
Cellule characteristics:	
Airfoil section	N-22
Dihedral, upper wing	1.0°
Dihedral, lower wing	0°
Sweepback, upper wing	7.2°
Sweepback, lower wing	0°
Gap (average)	6.25 ft.

TABLE II

ORIFICE LOCATIONS

Rib	Orifice location, inches back of leading edge													
	1	2	3	4	5	6	7	8	9	10	11	12	13	14
B_L	1.1	2.1	3.5	7.0	13.0	26.0	41.9	62.0						
A_L	1.0	2.0	3.5	7.0	12.9	22.9	34.9	48.0						
A_R	1.1	2.0	3.5	7.0	13.0	22.9	34.9	48.0						
B_R	1.1	2.1	3.5	7.0	13.0	26.0	42.0	62.1						
C	1.1	2.1	3.5	7.0	13.0	26.0	42.0	62.1						
D	1.2	2.1	3.6	7.1	13.1	25.0	40.0	55.1	61.3	64.4	67.4	70.4		
E	1.5	3.1	5.0	13.0	33.0	54.0	60.4	67.4						
F	2.5	3.7	5.2	8.7	14.7	24.7	35.7	43.7						
J_L	1.1	2.1	3.5	6.0	13.0	24.0	38.0	52.0						
H_L	1.0	2.1	3.6	6.1	13.0	24.0	38.0	51.9						
H_R	1.1	2.1	3.5	6.0	13.0	24.1	38.1	52.1						
J_R	1.0	2.0	3.5	6.0	13.0	24.0	38.0	52.0						
K	1.1	2.1	3.6	6.0	13.0	24.0	38.0	52.0						
L	1.1	3.1	6.1	15.1	33.1	48.0	54.0	60.0						
M	1.2	3.1	6.2	15.1	27.6	47.1	53.1	59.1						
N	1.7	2.7	4.7	7.7	11.1	19.1	25.2	35.1						
O	2.5	4.6	8.4	18.4	29.7	40.6	46.6	51.6	59.2	67.3				
P	2.2	3.7	6.1	11.3	22.4	28.3	31.2	33.2	38.9	42.2	46.4	51.3	56.3	61.2
Q	2.1	3.7	12.2	20.3	24.2	29.5	33.8	41.6	49.7					
R	2.0	3.5	6.0	11.5	15.8	23.8	29.8							

TABLE III

VARIATION OF $C_{D_{min}}$ WITH REYNOLDS NUMBER

$C_{D_{min}}$	R	Source	Elevator position (deg.)	Propeller condition
0.0520	2.8×10^6	F.S.T.	Tail off	Removed
.0565	2.8	"	0	"
.0555	2.8	"	5	"
.0560	2.8	"	10	"
.0565	2.8	"	15	"
.0545	5.05	"	6	"
.0650	2.8	"	9.65	Locked
.0640	5.05	"	8.15	"
.0620	13.1	Flight	-	"
.0615	4.89	F.S.T.	7.45	$\frac{nD}{V} = 0.979$
.0610	11.75	Flight	-	$\frac{nD}{V} = 0.985$

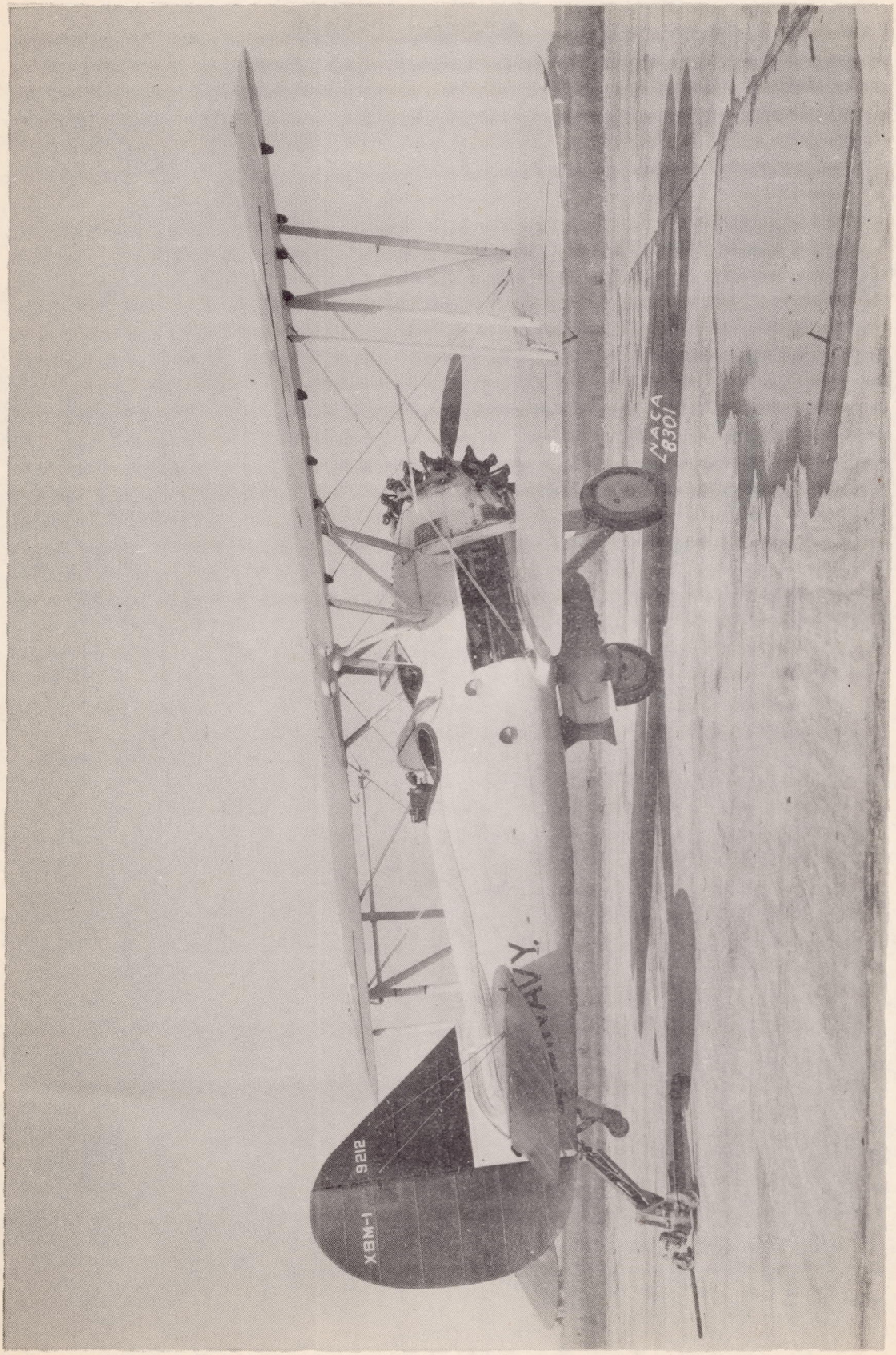

Figure 1.- The XBM-1 airplane.

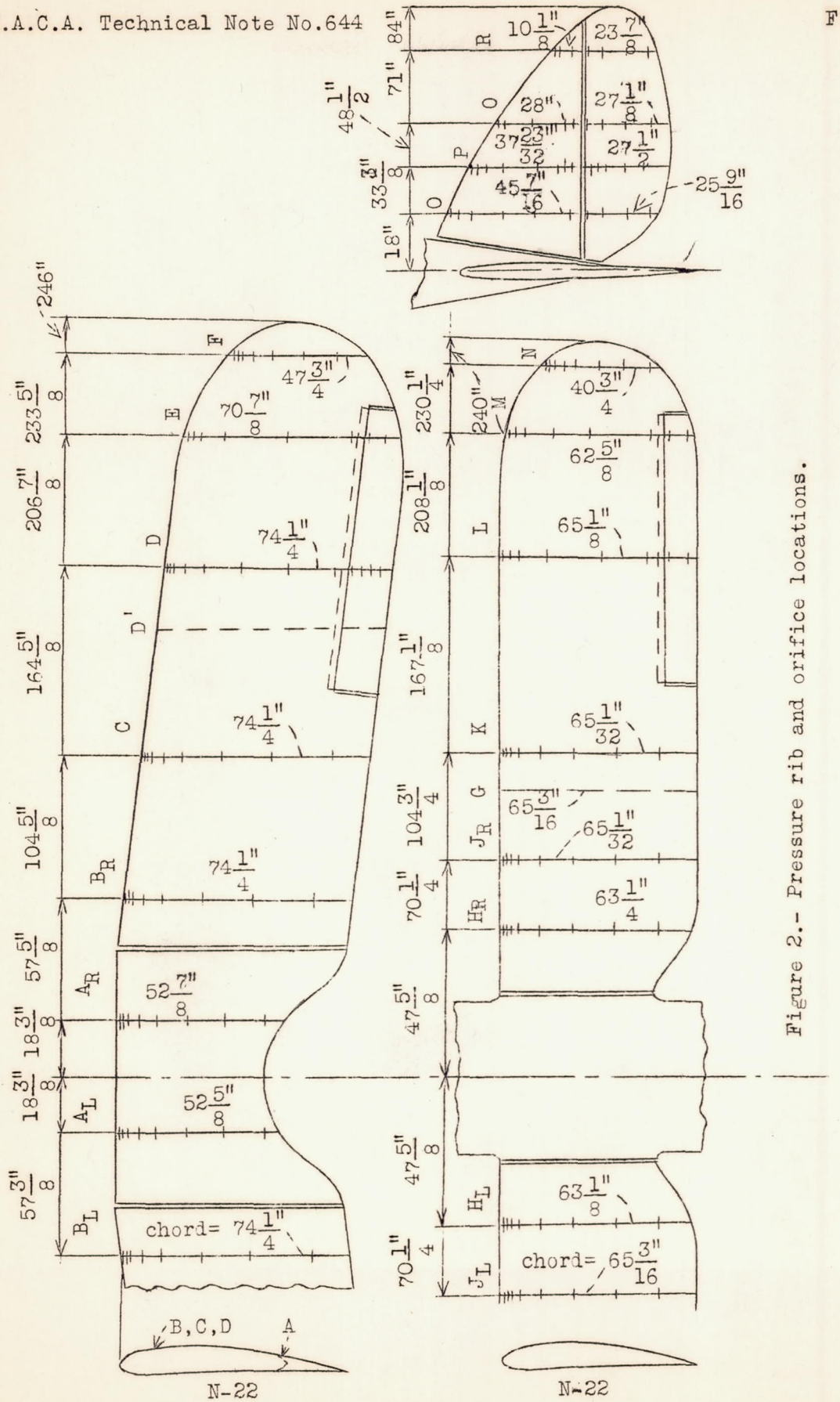

Figure 2.- Pressure rib and orifice locations.

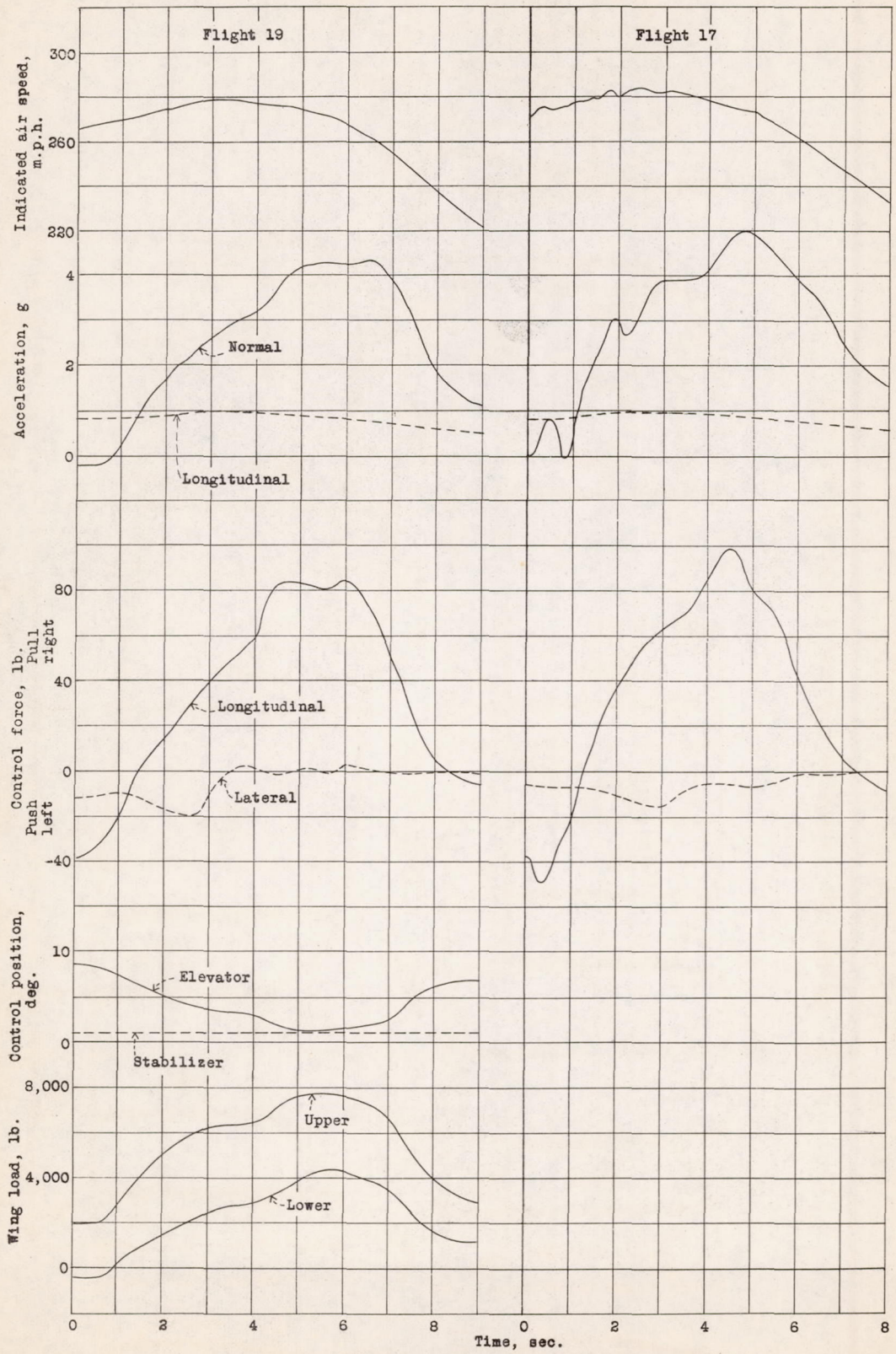

Figure 3.- Time histories of dive pull-outs (original wings).

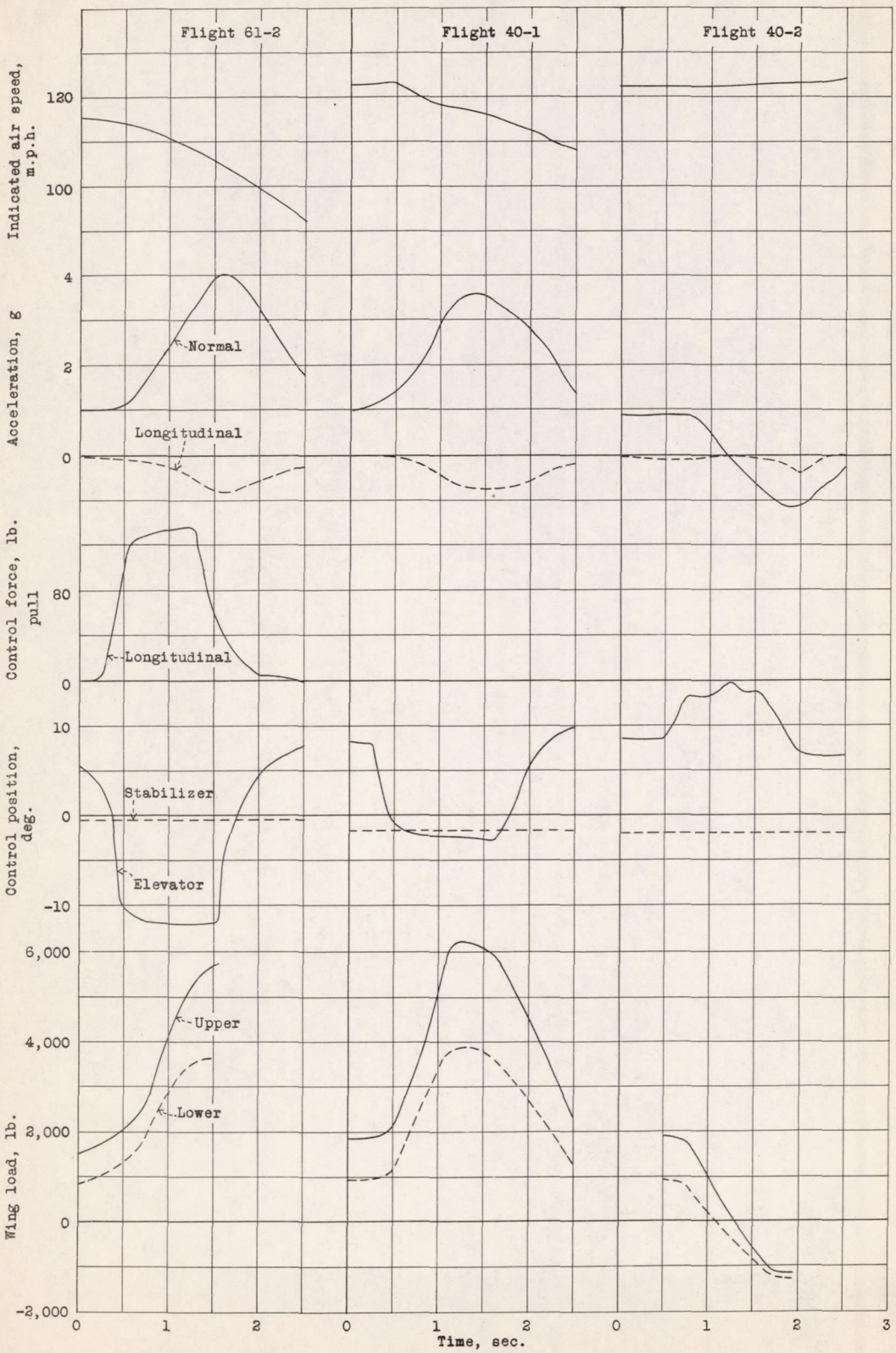

Figure 4.- Time histories of pull-ups and push-downs from level flight (original wings).

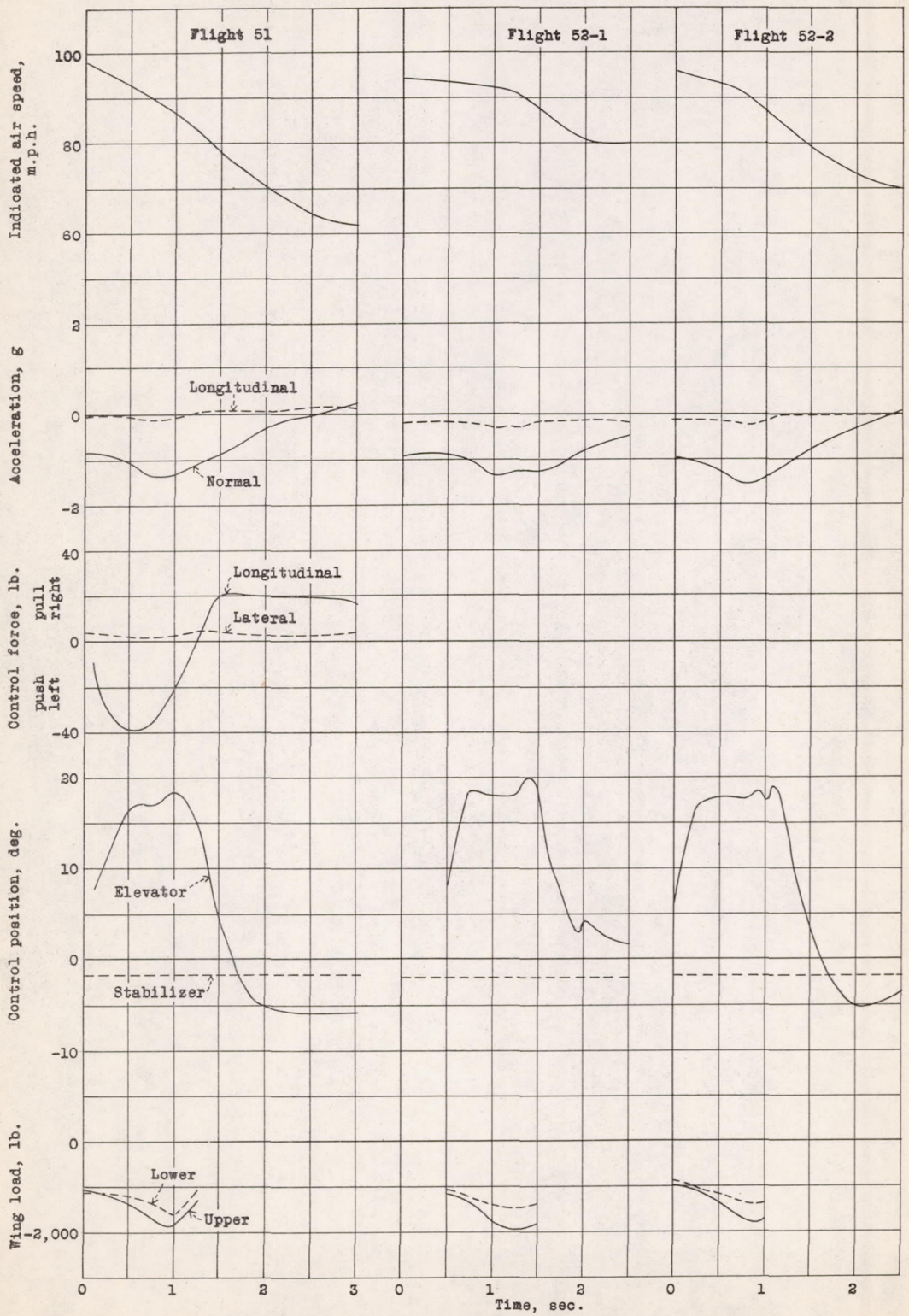

Figure 5.- Time histories of three inverted push-ups from level flight (original wings).

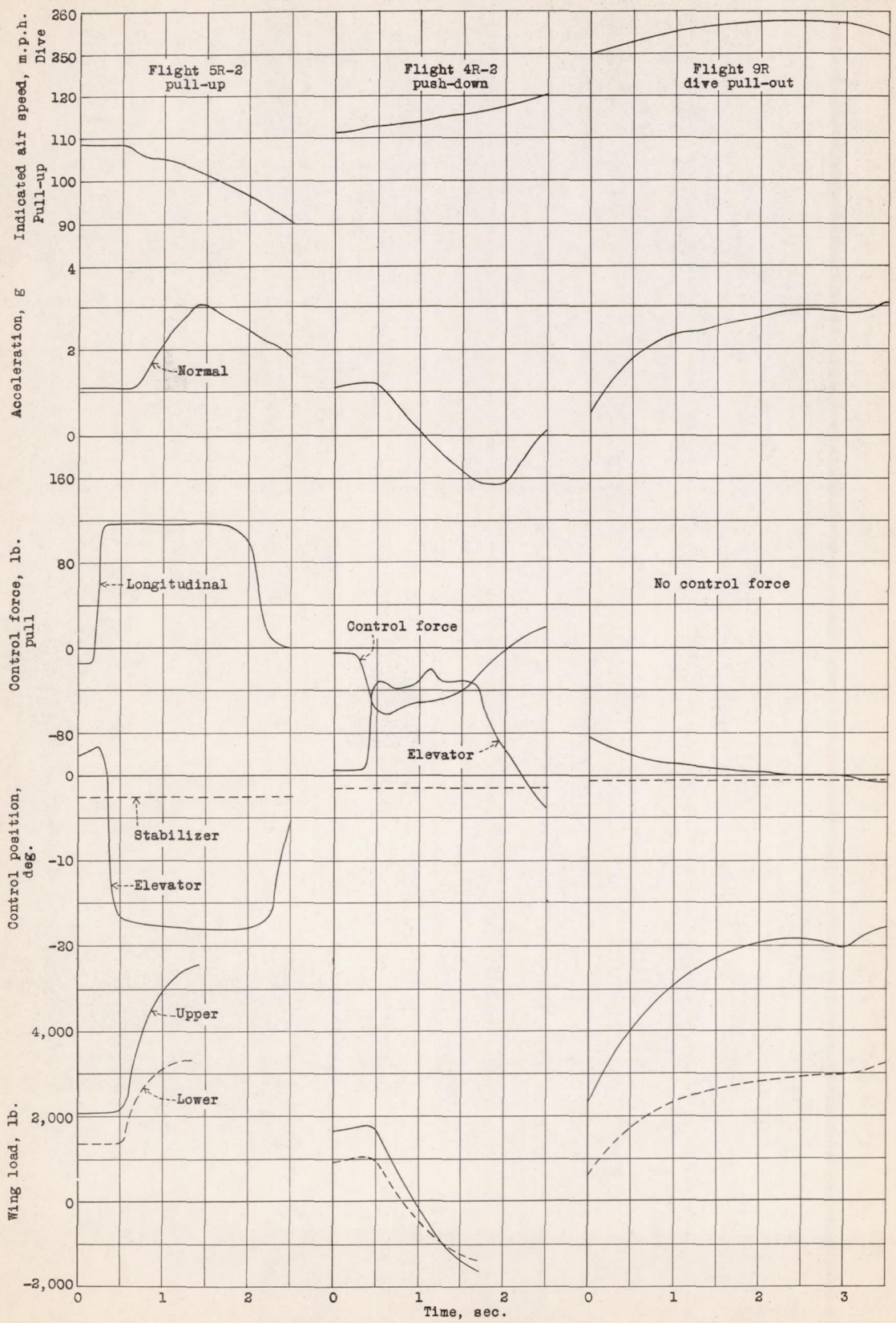

Figure 6.- Time histories of a pull-up, a push-down, and a dive pull-out (modified wings).

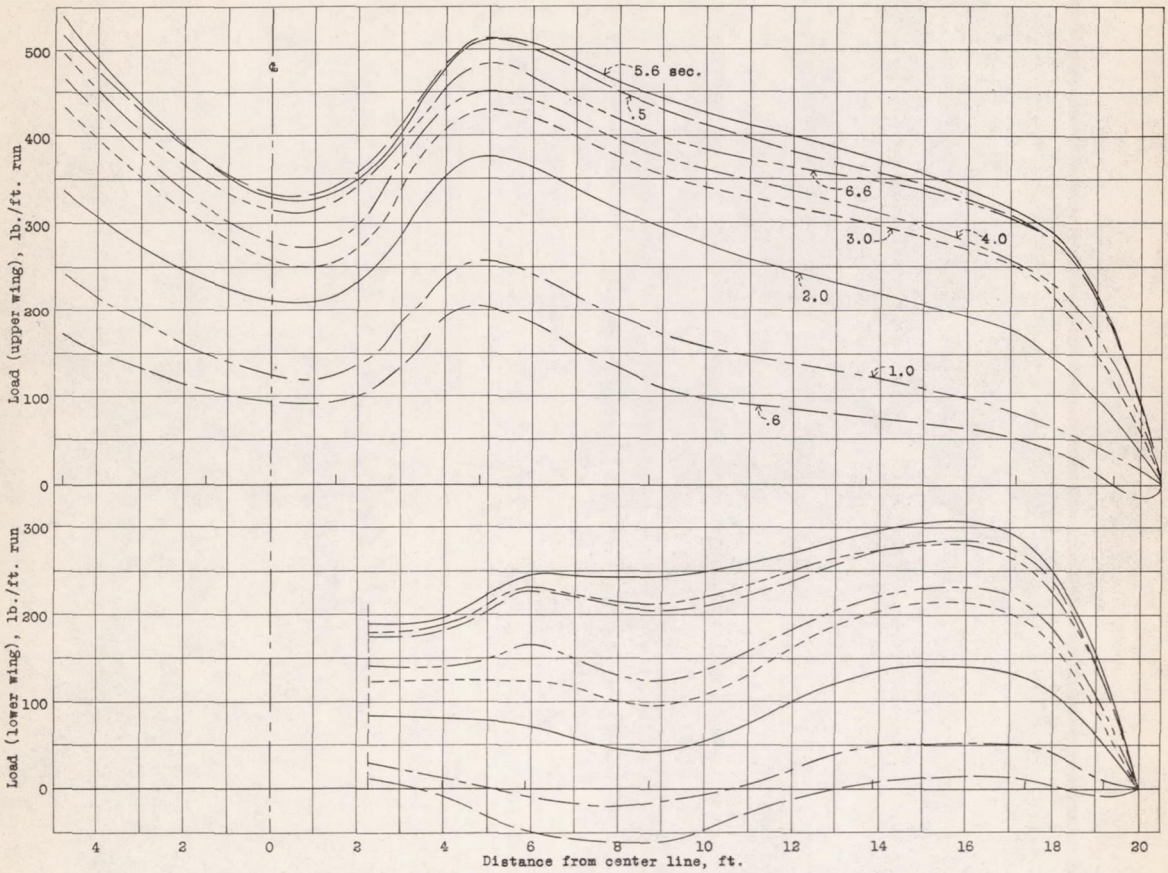

Figure 7.- Variation of load distribution during a dive pull-out (flight 19, original wings).

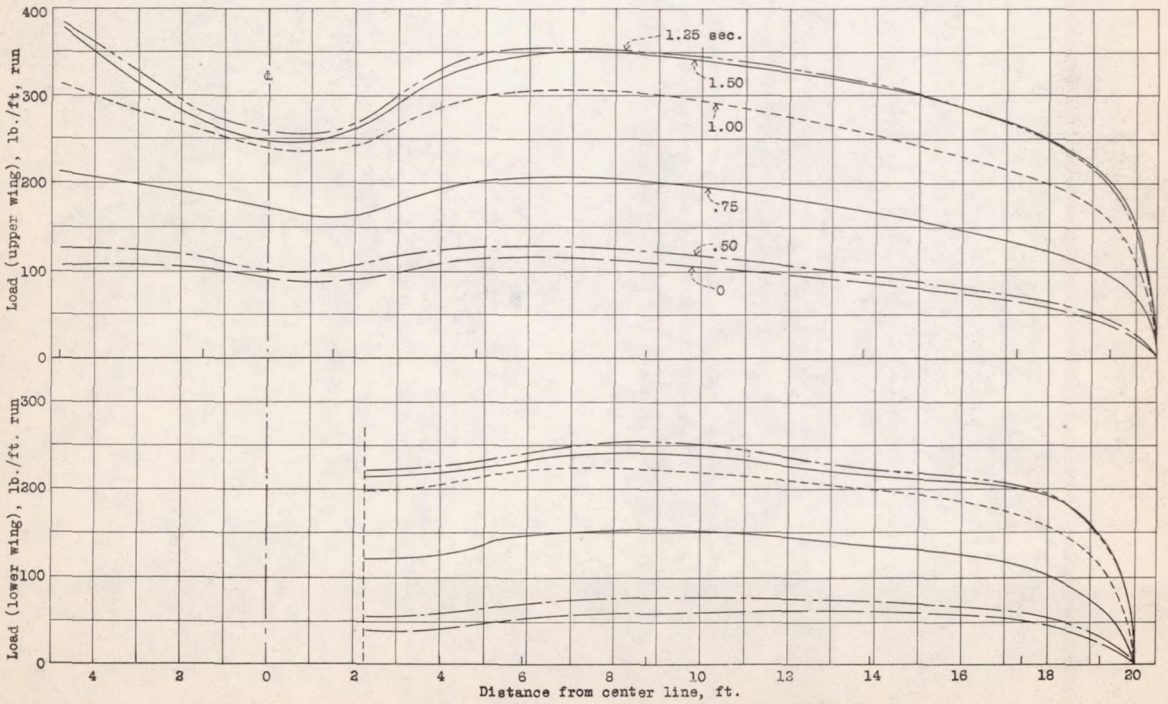

Figure 8.- Variation of load distribution during a pull-up (flight 40-1, original wings).

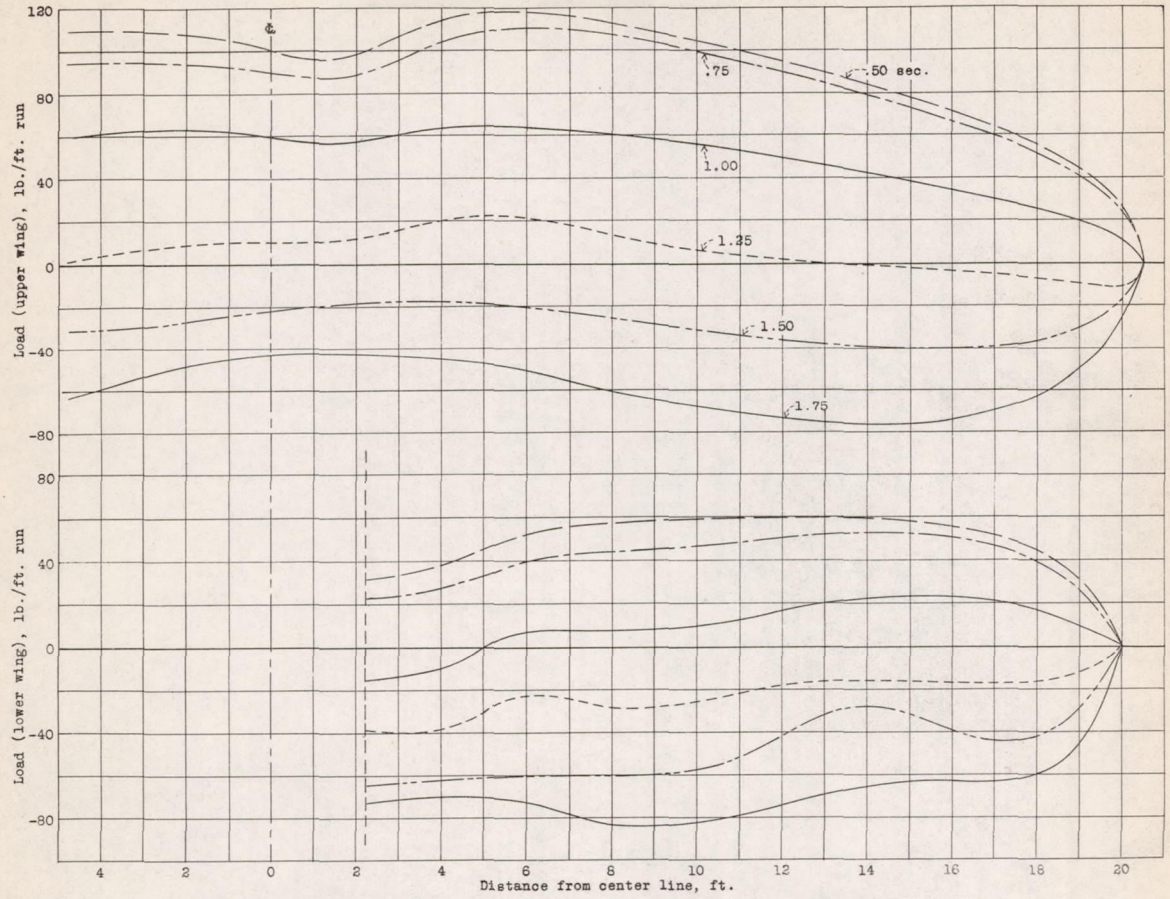

Figure 9.- Variation of load distribution during a push-down (flight 40-2, original wings).

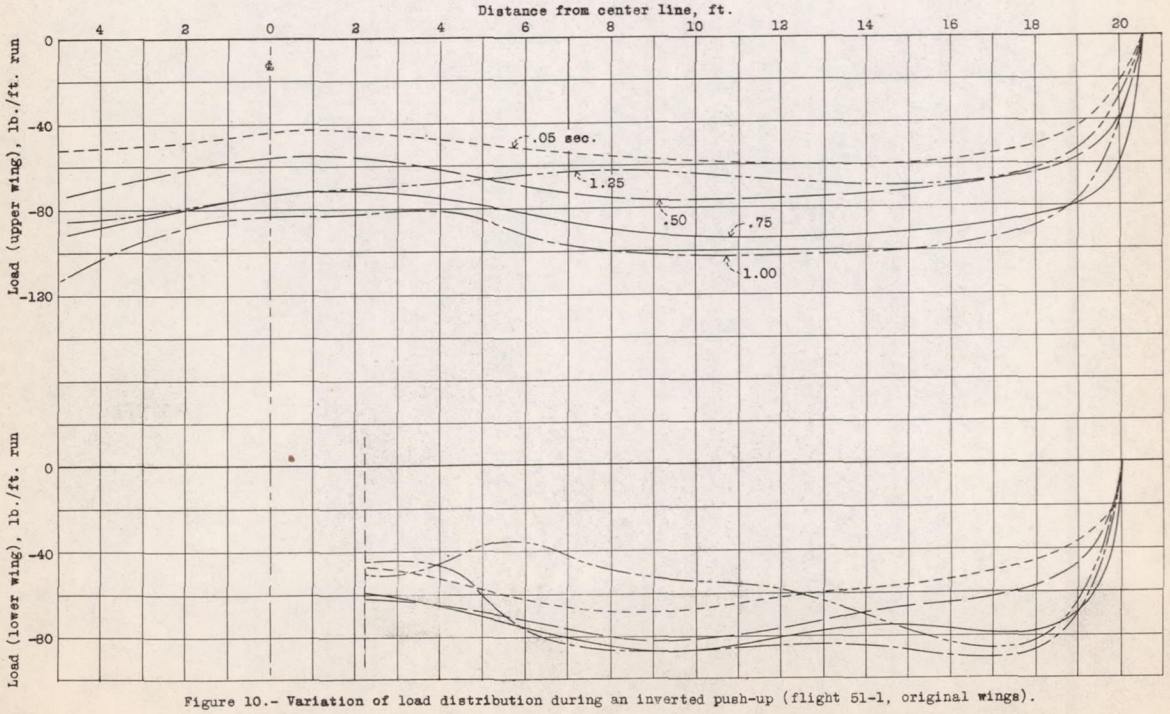

Figure 10.- Variation of load distribution during an inverted push-up (flight 51-1, original wings).

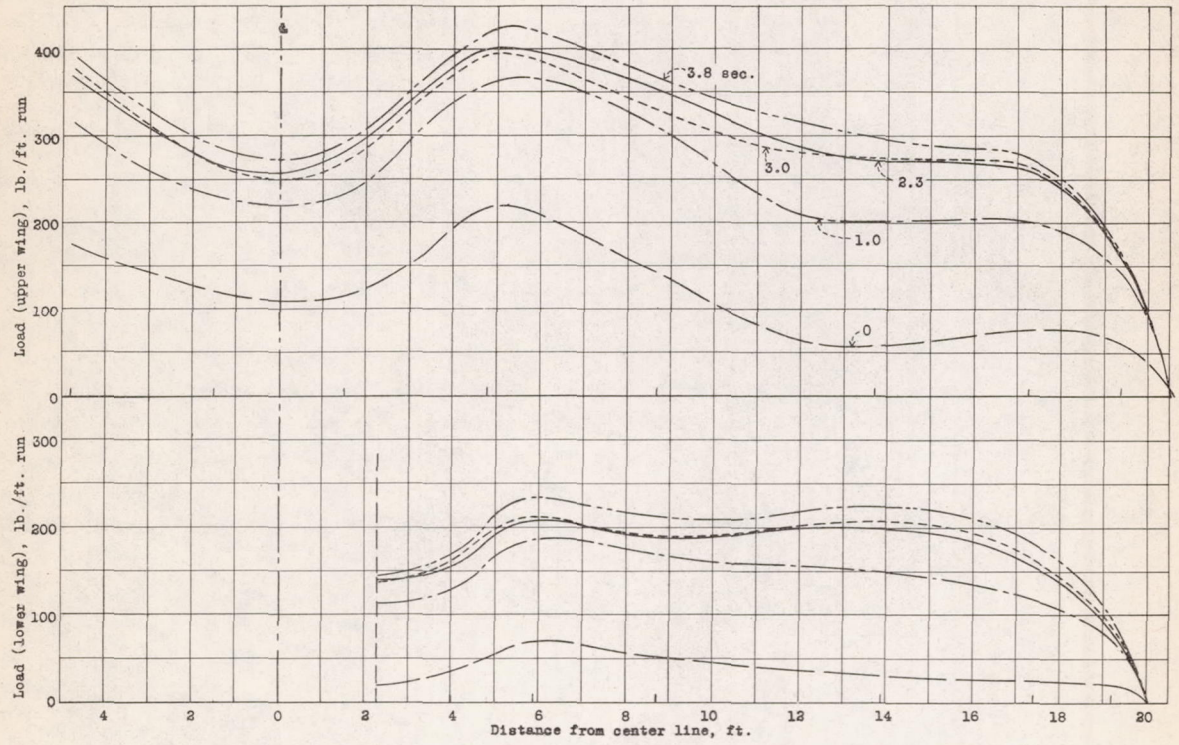

Figure 11.- Variation of load distribution during a dive pull-out (flight 9R, modified wings).

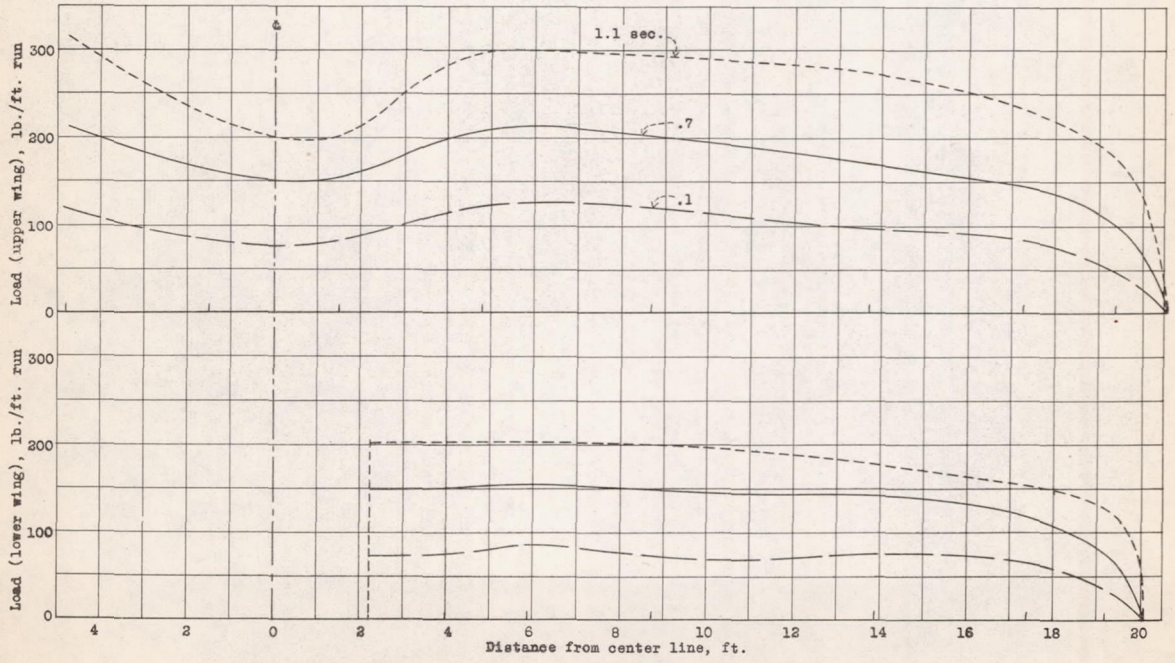

Figure 12.- Variation of load distribution during a pull-up (flight 5R-1, modified wings).

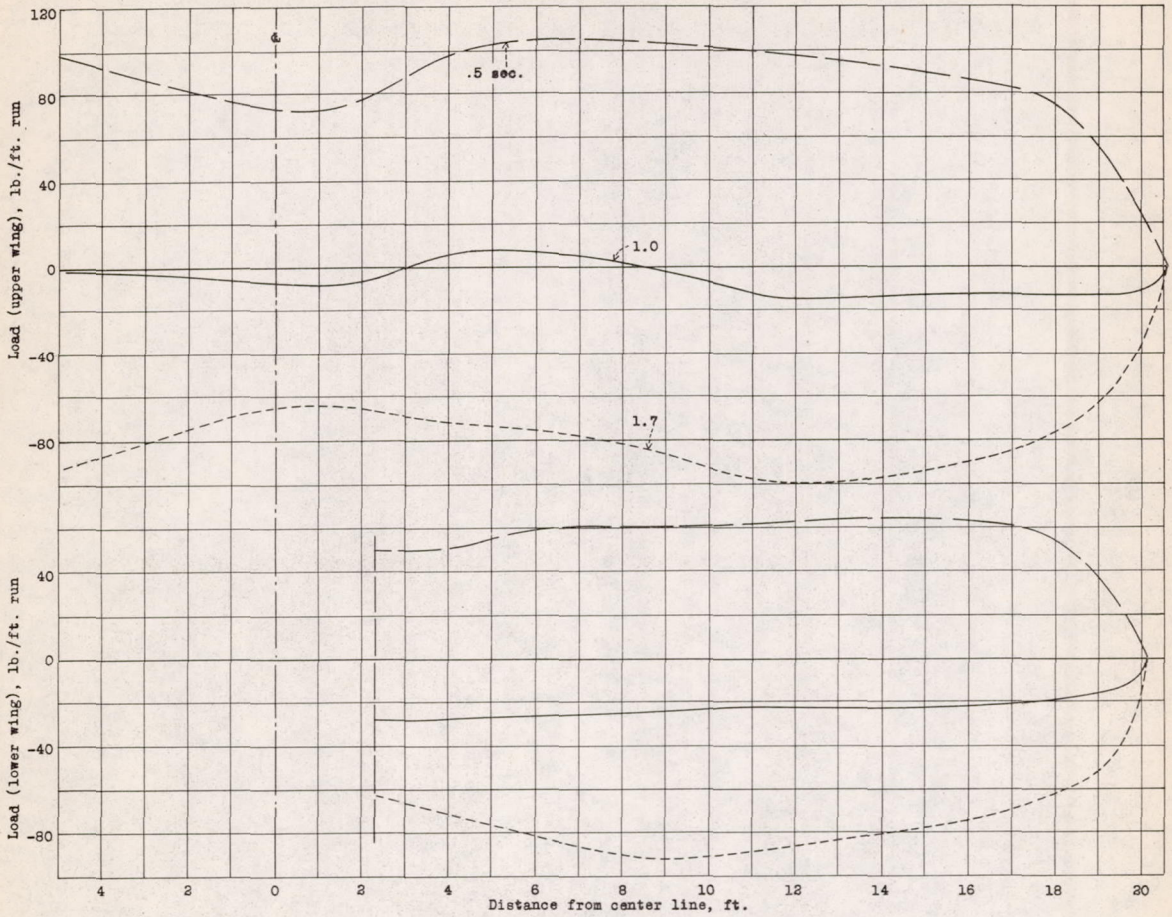

Figure 13.- Variation of load distribution during a push-down (flight 4R-2, modified wings).

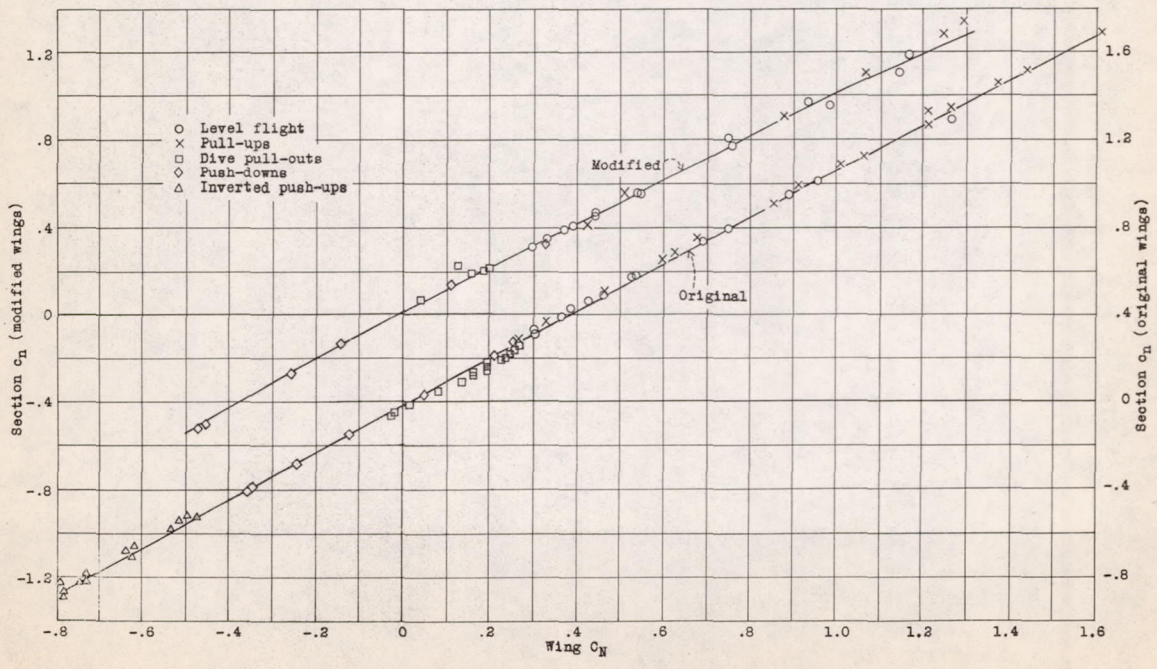

Figure 14.- Variation of section c_n with wing C_N (rib K).

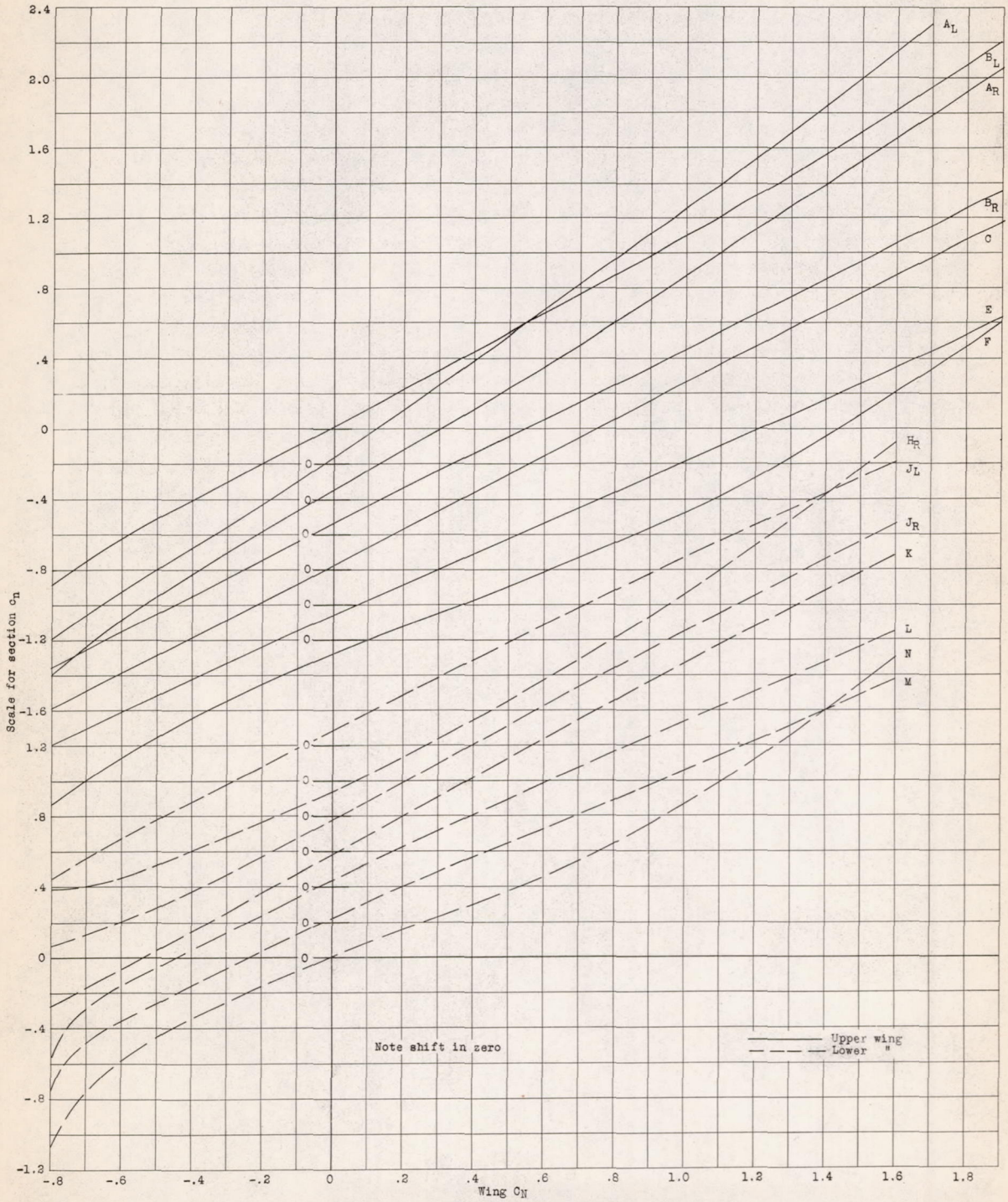

Figure 15.- Variation of section c_n with wing C_N (original wings).

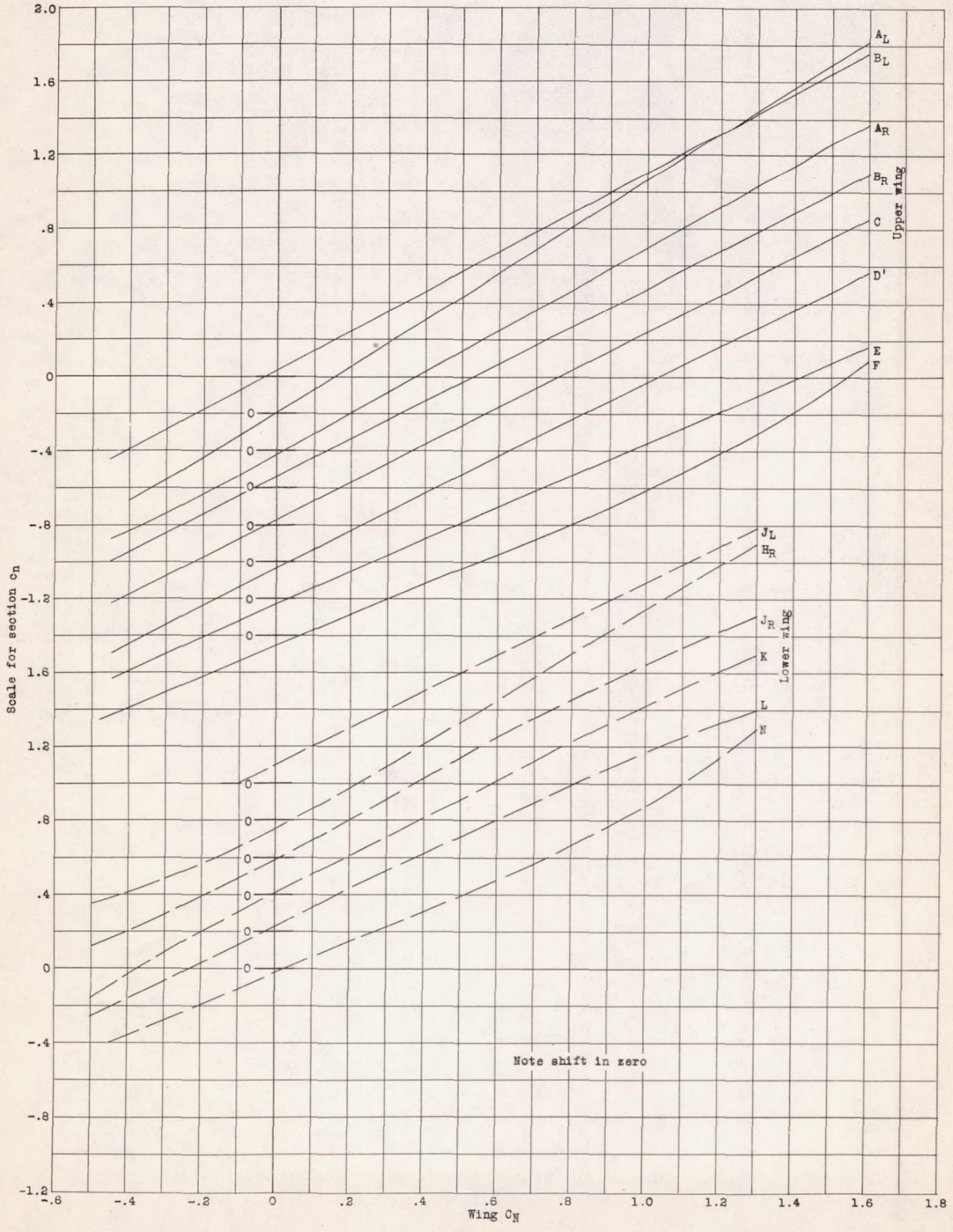

Figure 16.- Variation of section c_n with wing C_N (modified wings).

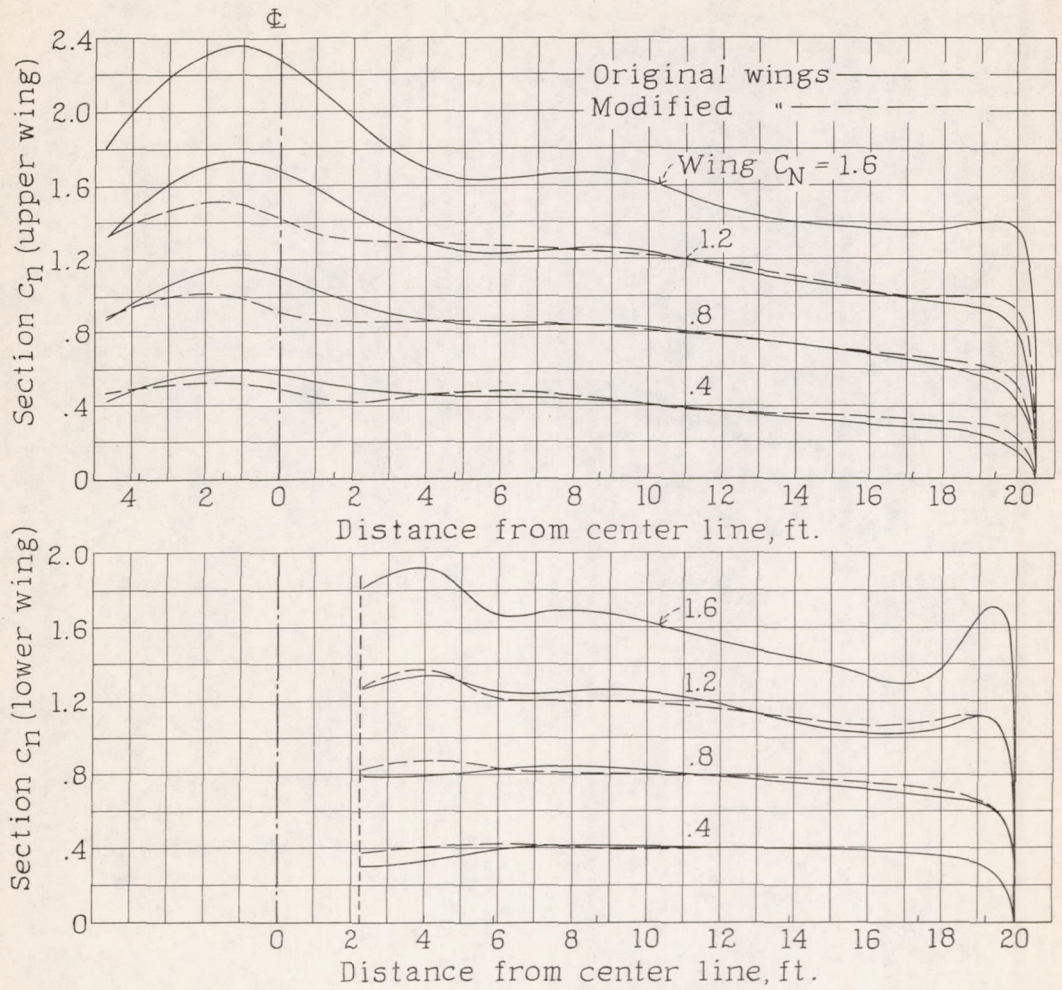

Figure 17.- Comparison of average section c_n values for original and modified wings.

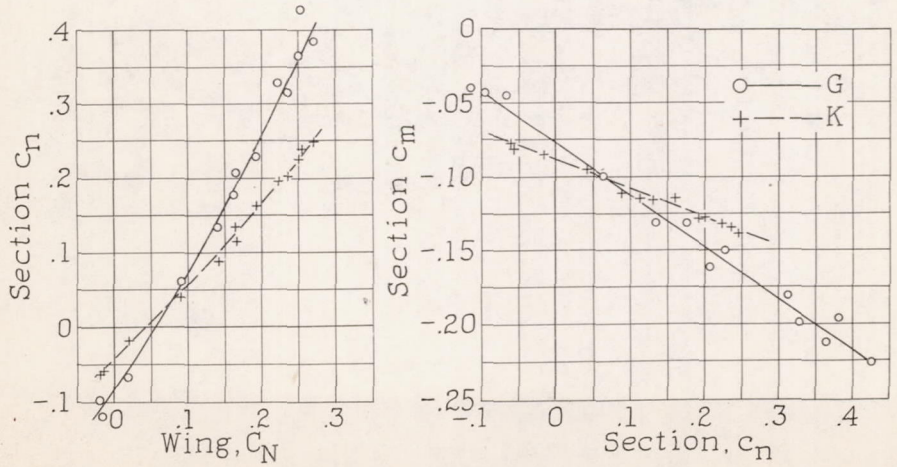

Figure 22.- Comparison of relations for floating rib G with those of rib K.

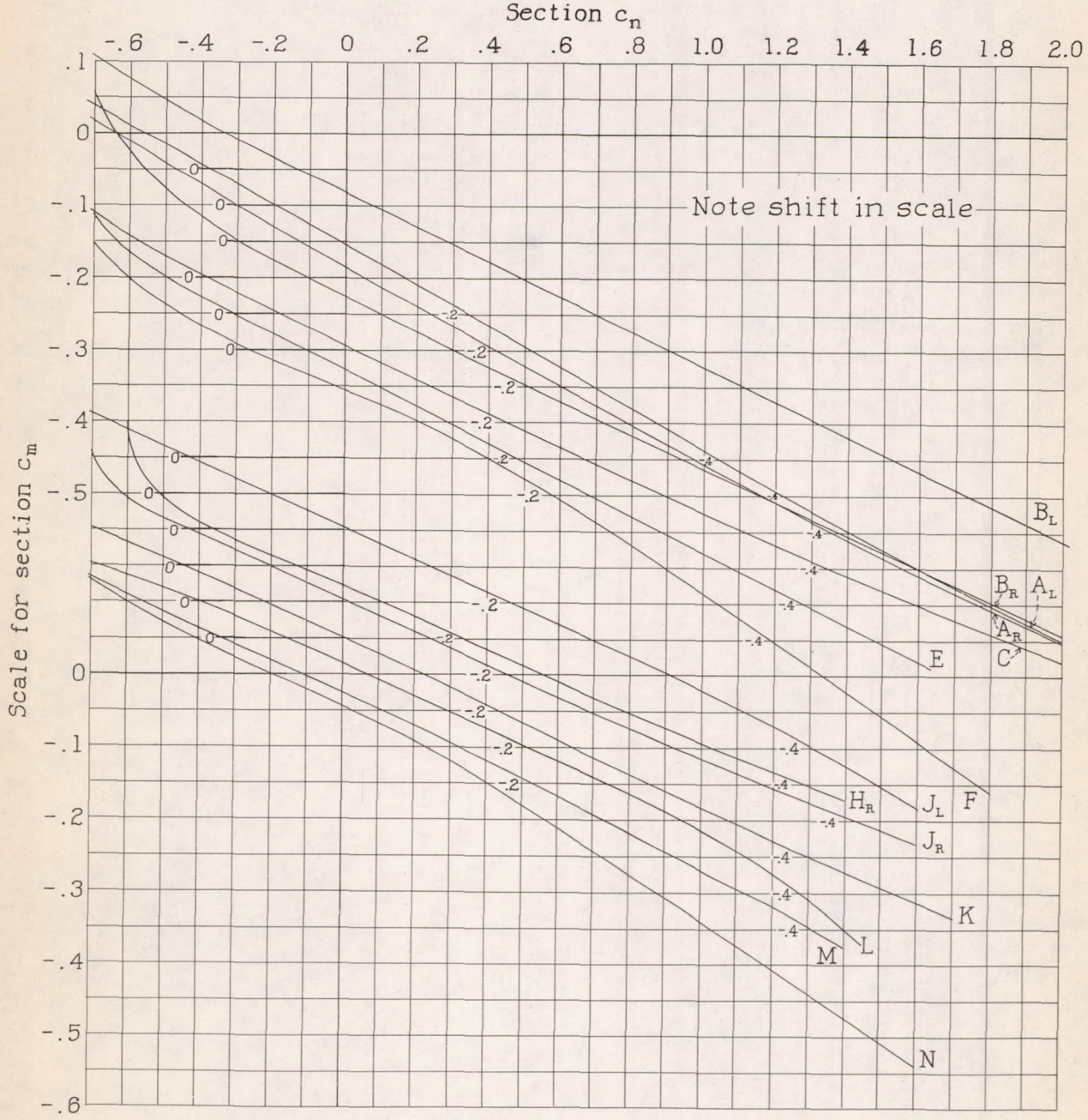

Figure 18.- Variation of section c_m with section c_n (original wings).

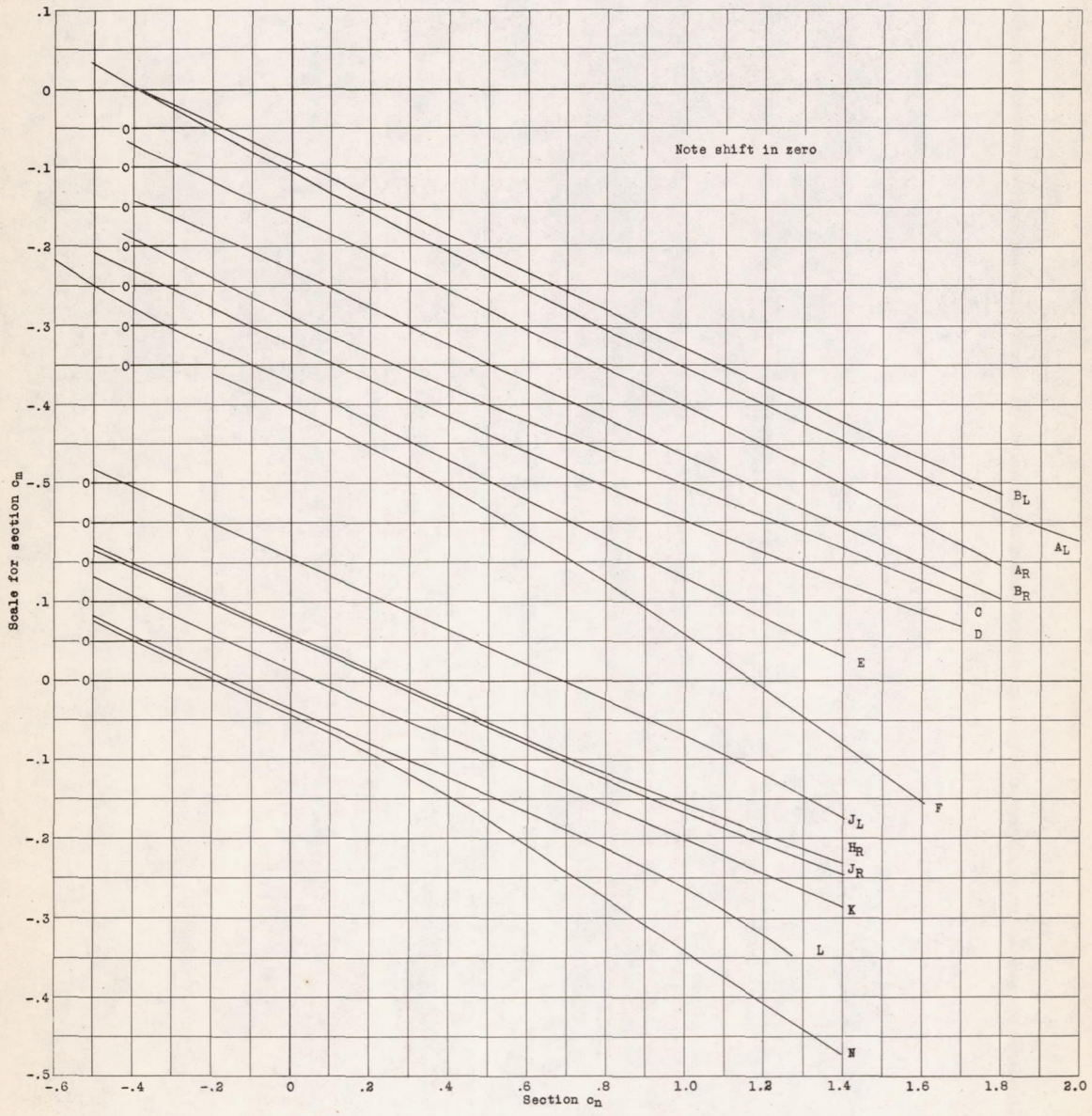

Figure 19.- Variation of section c_m with section c_n (modified wings).

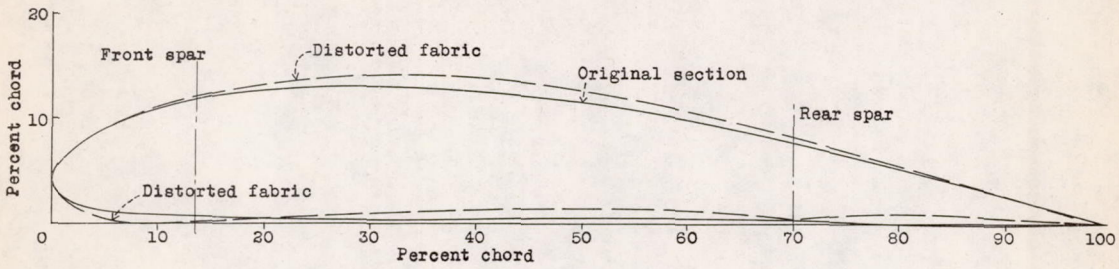

Figure 21.- Section profile distortion during a dive pull-out.

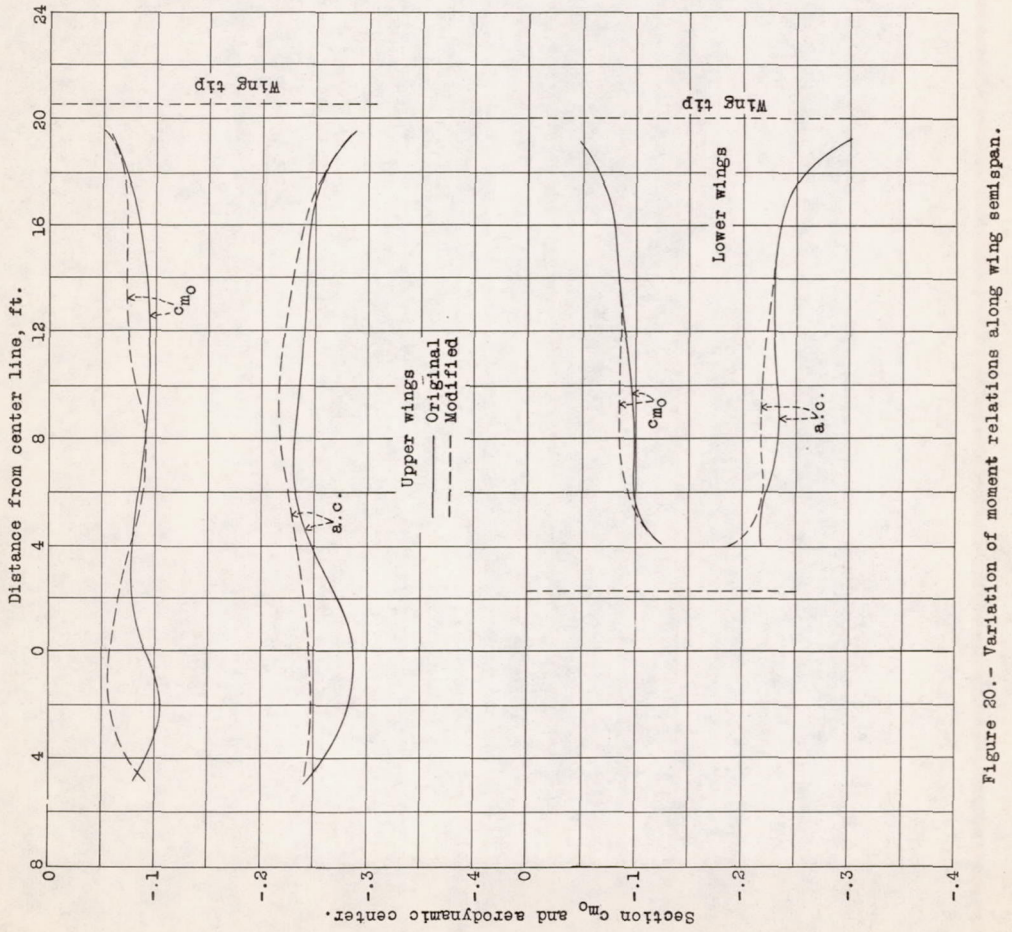

Figure 20.- Variation of moment relations along wing semispan.

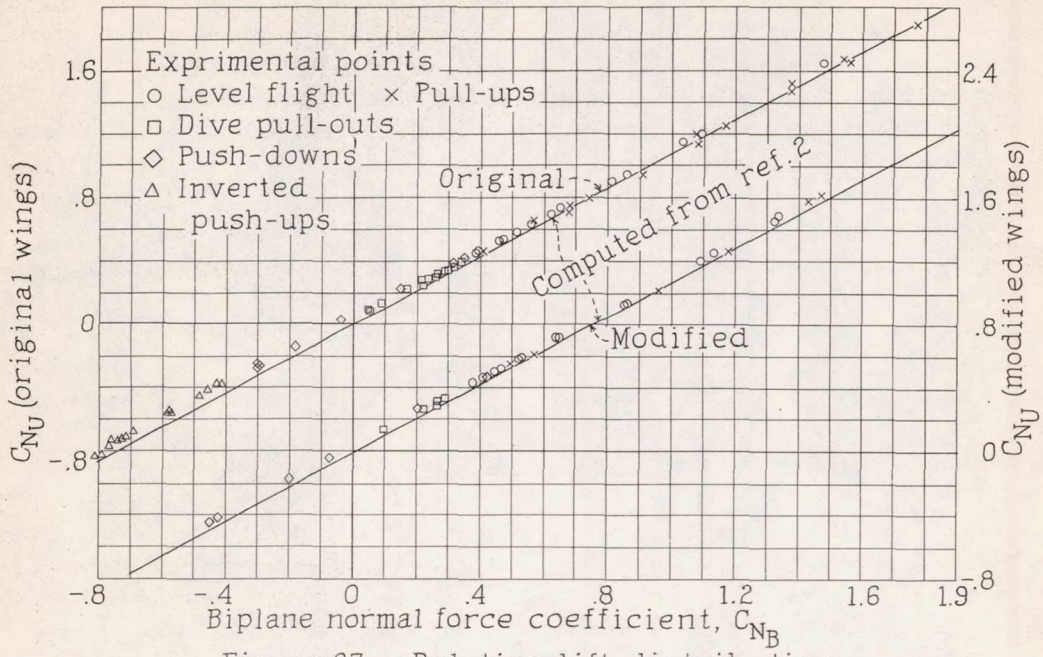

Figure 23.- Relative lift distribution.

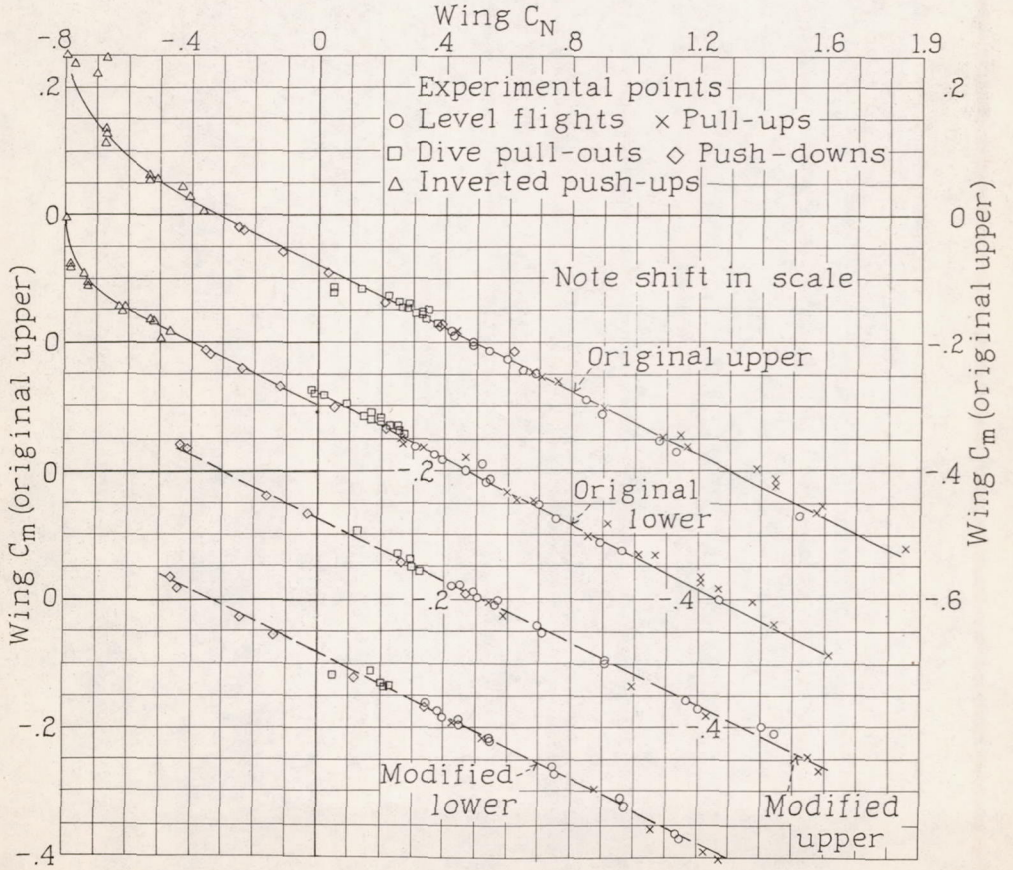

Figure 24.- Variation of wing C_m with wing C_N

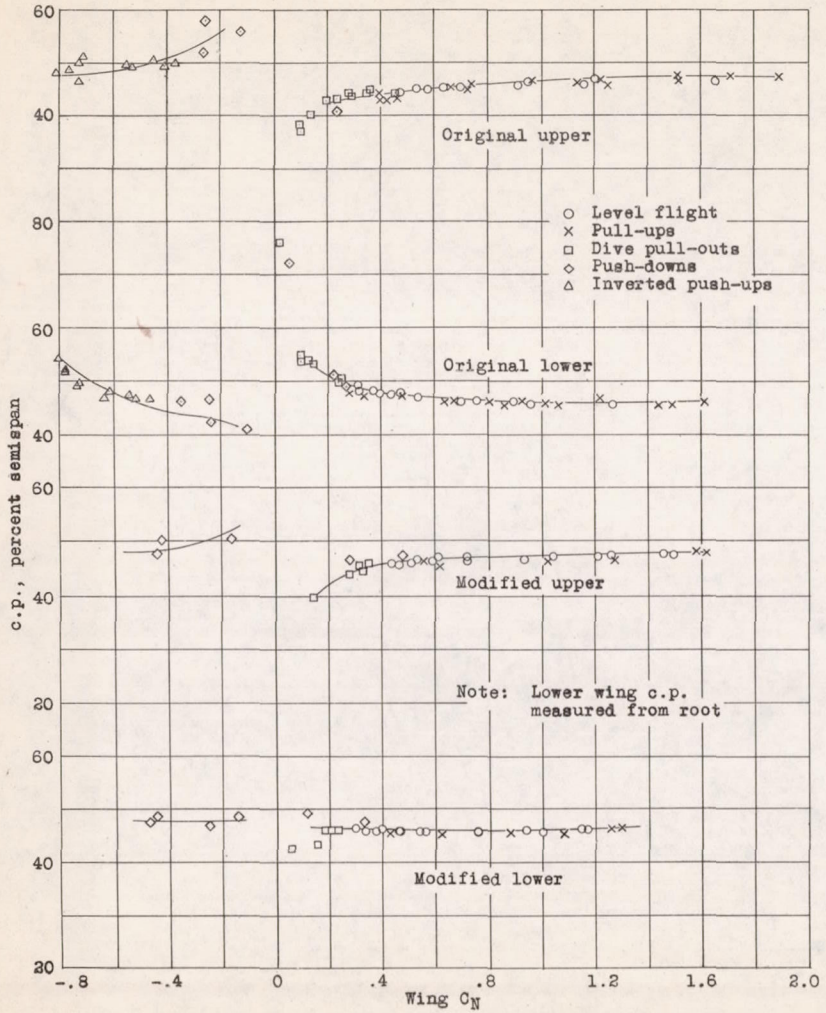

Figure 25.- Variation of lateral centers of pressure with wing C_N.

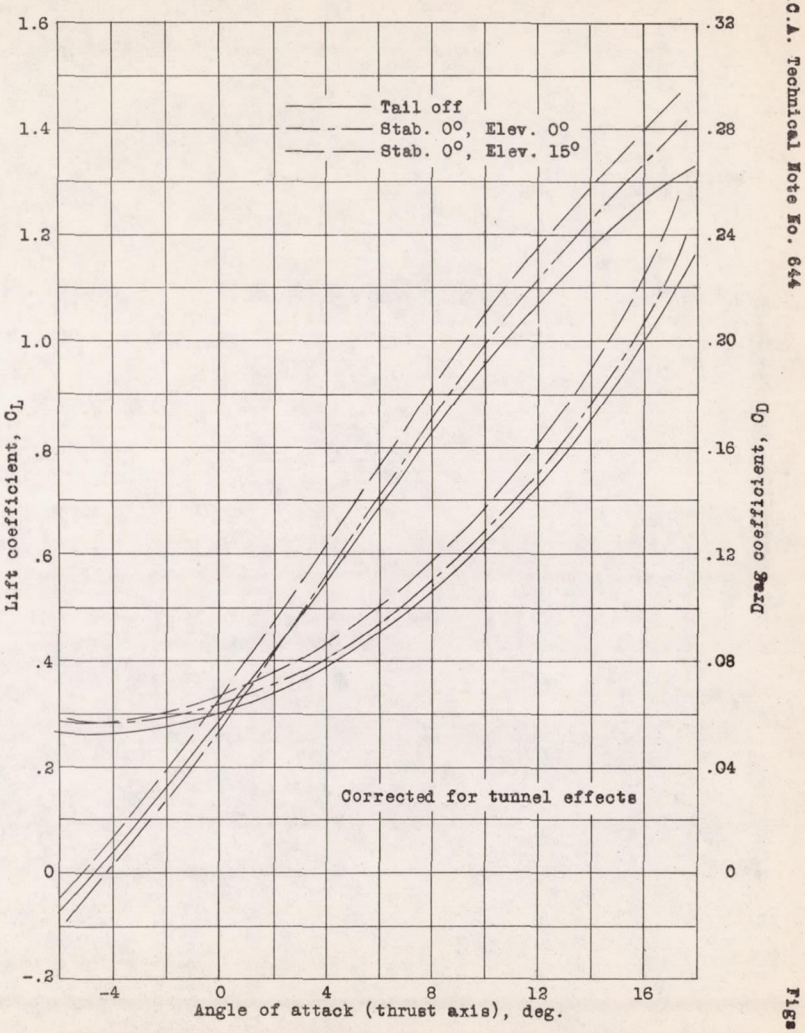

Figure 26.- Lift and drag coefficients for the XBM-1 airplane measured in the full-scale tunnel.

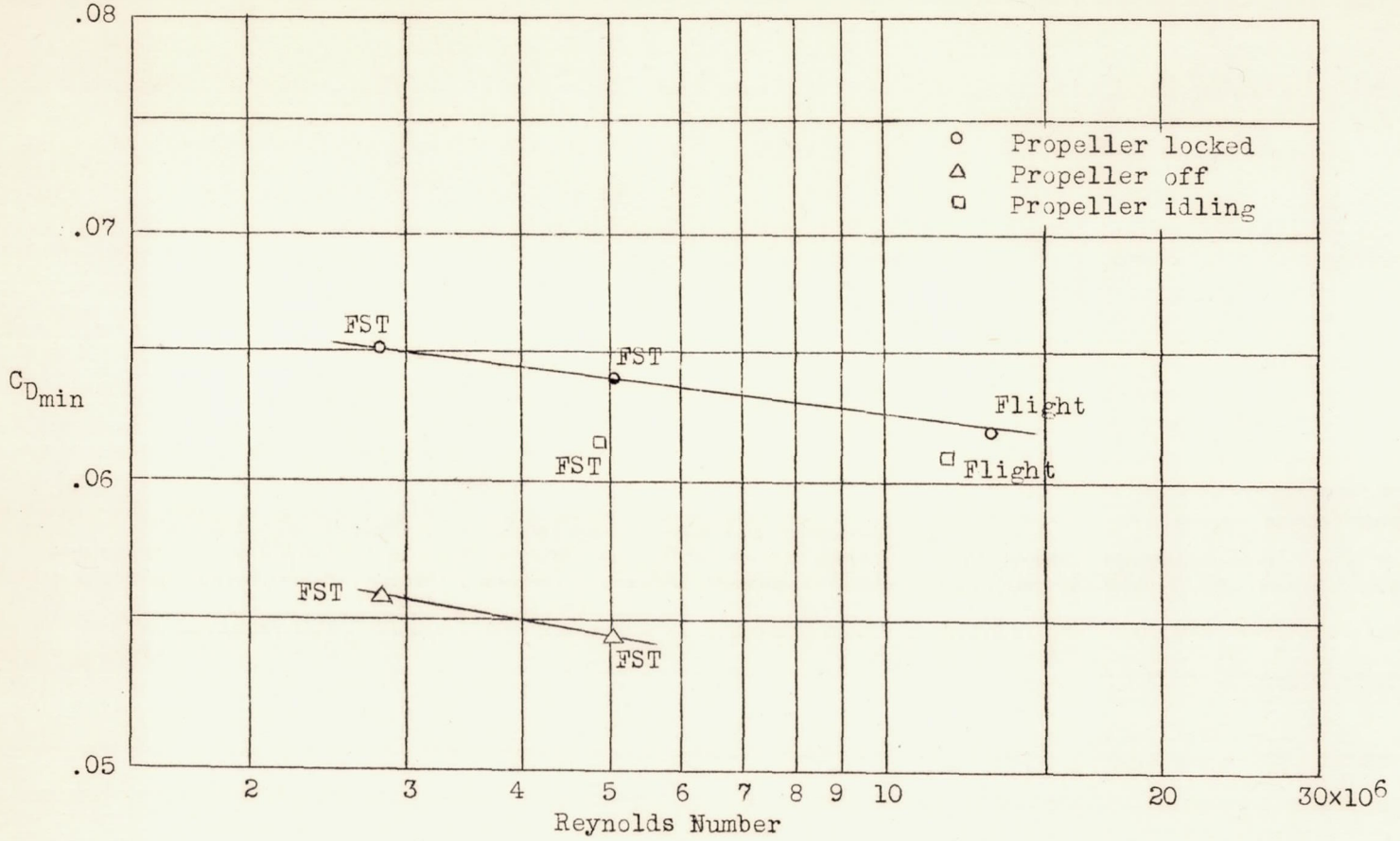

Figure 27.- Variation of $C_{D_{min}}$ with Reynolds Number.

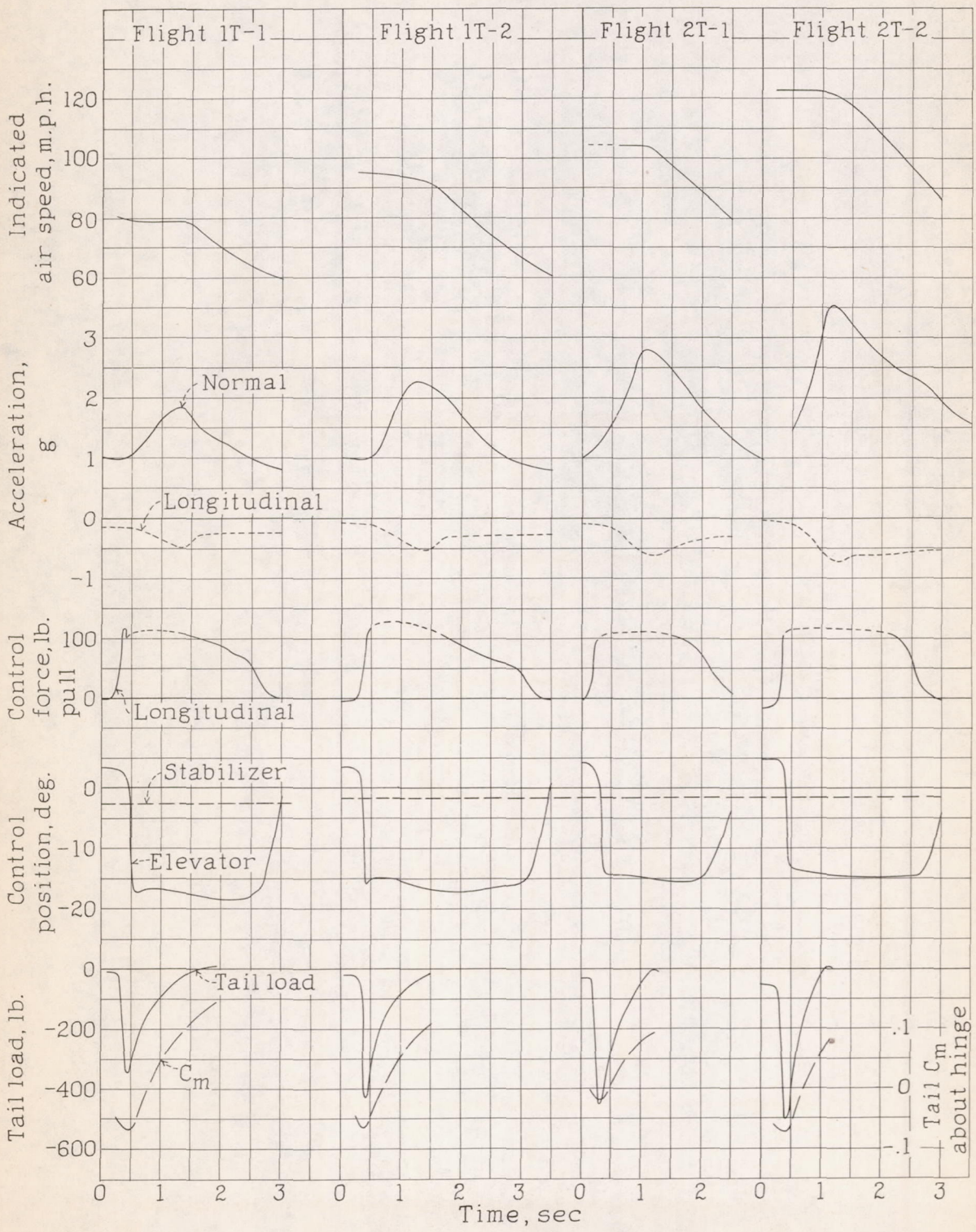

Figure 28.- Time histories of pull-ups at various speeds.

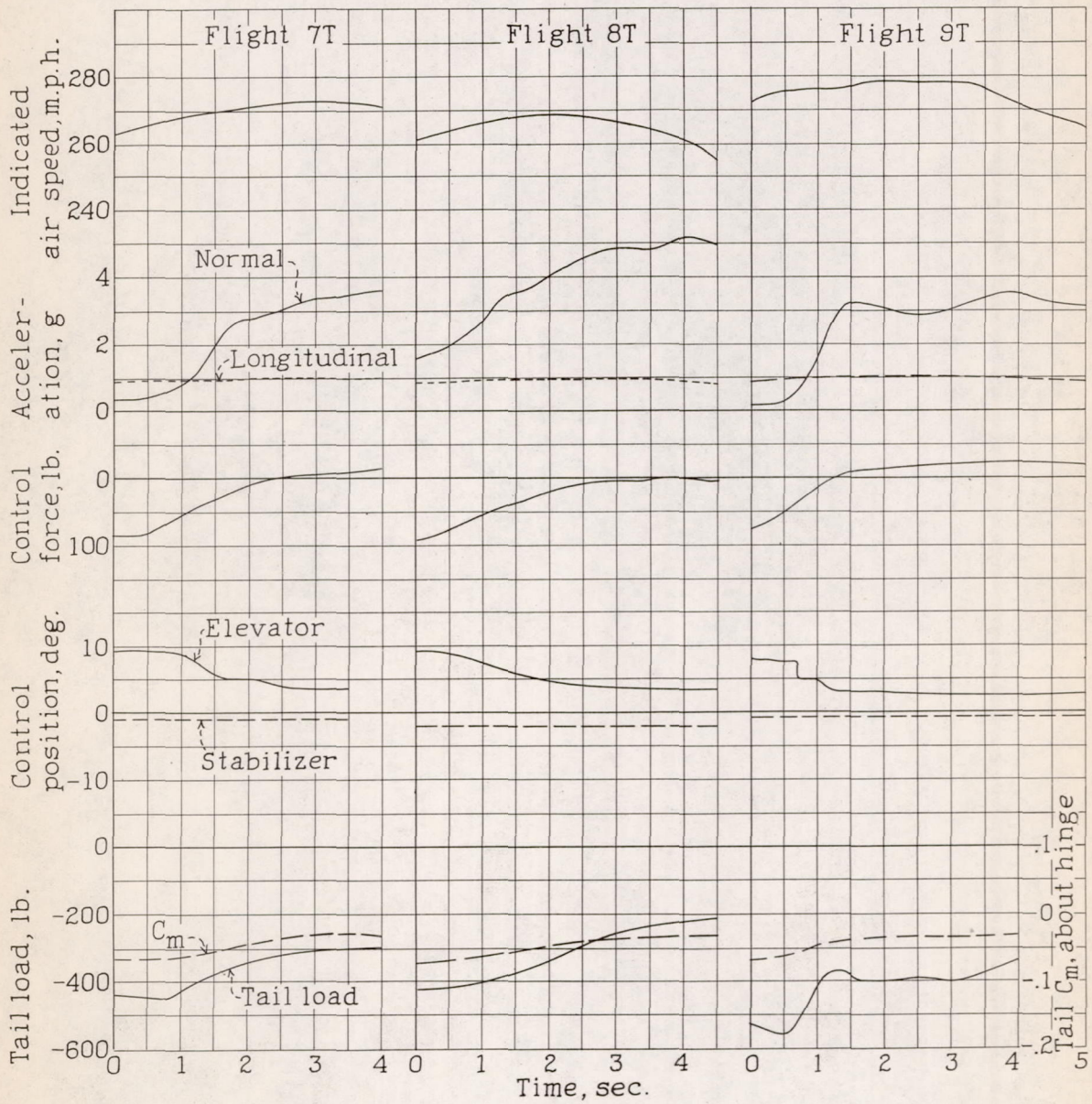

Figure 29.- Time histories of dive pull-outs.

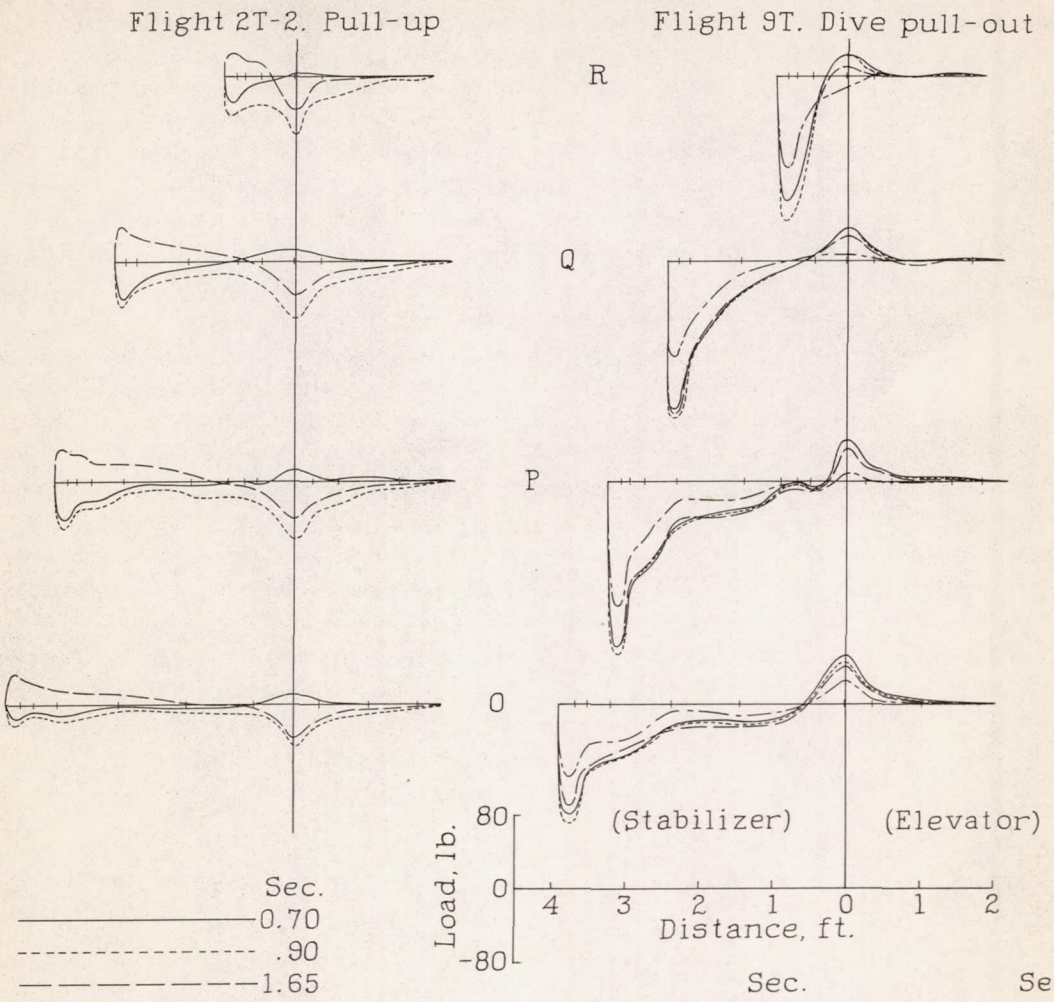

Figure 30.- Distribution of rib loading during a pull-up and a dive pull-out.

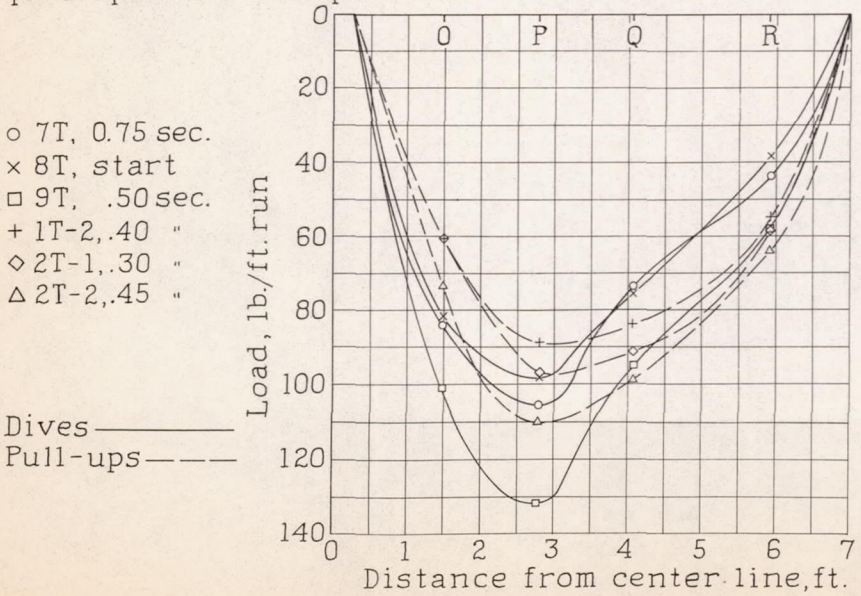

Figure 31.- Variation of tail load distributions at maximum load.